Student thesis series INES nr 304

Polynomial trends of vegetation phenology in Sahelian to equatorial Africa using remotely sensed time series from 1983 to 2005

Mozafar Veysipanah

2014
Department of
Physical Geography and Ecosystems Science
Lund University
Sölvegatan 12
S-223 62 Lund
Sweden

Mozafar Veysipanah (2014). Polynomial trends of vegetation phenology in Sahelian to equatorial Africa using remotely sensed time series from 1983 to 2005

Master degree thesis, 30 credits in *Physical geography*

Department of Physical Geography and Ecosystems Science, Lund University

Seminar series nr 304

Mozafar Veysipanah

Master thesis, 30 credits, in Physical geography and ecosystem analysis

Supervisor:

Prof. Lars Eklundh

Department of Physical Geography and Ecosystem Science
Lund University

Mars 2014

Abstract

Global warming has both short and long term effects on seasonal phenological cycles of vegetation. Phenology parameters of vegetation such as start, end, length and amplitude of season can describe life cycle events of vegetation. These parameters are commonly extracted from vegetation indices. Long-term dataset of GIMMS NDVI time series from 1983 to 2005 was used to extract and analyze vegetation phenology over Sahelian to equatorial areas. TIMESAT software package was used as an automated method to extract the phenology parameters of the dataset. Since changes of vegetation are not always simply linear; higher order of polynomial trends was applied to investigate the fluctuation of phenology parameters using methodology developed by Jamali et al. (2014). A new concept denoted "polynomial hidden trends" was introduced by Jamali et al. (2014), referring to areas with no significant linear changes, while they can be described by significant higher order polynomials.

Results showed that the polynomial trends can detect notable proportions of vegetation changes over the study area, although changes of phenology parameters were mainly explained by linear trends. Also, a significant portion of the change was represented through quadratic and cubic trends.

Since soil moisture is identified as a better indicator than rainfall to describe vegetation greenness (Huber et al., 2011), polynomial trends in soil moisture were compared against mean values of dates of occurrence of phenology parameters. There were several other factors influencing vegetation phenology such as rainfall, land cover and soil texture. These factors also were compared against the results of each phenology parameter.

Results also illustrated that soil moisture trends followed the phenology parameters trends of Start of growing Season (SOS) and End Of growing Season (EOS). It was found that Entisols and Oxisols were associated with phenology changes, particularly in the Guinean zone. Also, deciduous woodland, shrub lands and irrigated crop lands were found to be those land covers with maximum response to variation in phenology parameters.

Acknowledgment

I would like to express my very great appreciation to my supervisor, Professor Lars Eklundh for his willingness to give his time so generously, valuable and constructive advice, recommendations and helpful ideas to improve my work in all the time of research and writing of this thesis.

I would also like to thank Jonathan Seaquist for his support and valuable comments from the beginning of my thesis work.

I am indebted to Sadegh Jamali for providing GIMMS NDVI data, for his technical support especially to learn TIMESAT, for using his polynomial algorithm and his written Matlab script and for his limitless help through my thesis.

I would like to thank Jonas Ardö for providing the rainfall station data. I am very thankful to Harry Lankreijer and Helena Erikson for the administrative help in order to study at Lund University.

I take this opportunity to express a deep sense of gratitude to all of my teachers and staff here in the Department of Physical Geography and Ecosystem Analysis for their assistance, kind hospitality and endless support during my studies in Lund University.

I would like to thank all of my friends and colleagues at the Department of Physical Geography and Ecosystem Analysis.

I would also like to thank all my family for supporting me during my life.

I also take this opportunity to express my deepest sense of gratitude and love to my wife, Kewsan Amini, who encouraged and supported me to continue my study.

Table of Contents

List of figures and tables

Figures

Tables:

Abbreviations

AMP (Amplitude of season)

AVHRR (Advanced Very High Resolution Radiometer)

BFAST (Breaks For Additive Season and Trend)

BISE (Best Index Slope Extraction)

CDAS (Coupled Data Assimilation System)

CPC (Climate Prediction Center)

DC/PAC (Desertification Control Programme Activity Centre)

DOY (Day Of Year)

EOS, EOS (End of Growing Season)

EMD (Empirical Mode Decomposition)

ESRI (Environmental Systems Research Institute)

EVI (Enhanced Vegetation Index)

FAO/GIEWS (FAO- Global Information and Early Warning System)

FAO (Food and Agriculture Organization)

GDP (Gross Domestic Production)

GEMS (Global Environment Monitoring System)

GIMMS (Global Inventory Monitoring and Modeling Systems)

GLC (Global Land Cover)

GRID (Global Resource Information Database)

IPCC (International Panel for Climate Change)

ITCZ (Inter-Tropical Convergence Zone)

LCCS (Land Cover Classification System)

LOS, LOS (Length of Growing Season)

LSP (Land Surface Phenology)

MODIS (Moderate Resolution Imaging Spectro-radiometer)

MRS (Mean Root Square)

MSAVI (Modified Soil-Adjusted Vegetation Index)

MVC (Maximum Value Composition)

NASA (National Aeronautics and Space Administration)

NDVI (Normalized Difference Vegetation Index)

NDWI (Normalized Difference Water Index)

NOAA (National Oceanic and Atmospheric Administration)

PAR (Photosynthetically Active Radiation)

SAVI (Soil-Adjusted Vegetation Index)

SOS, SOS (Start of Growing Season)

SI (Small Integral of season)

TAR (Third Assessment Report)

UNEP (United Nations Environment Programme)

UNESCO (United Nations Educational, Scientific and Cultural Organization)

UTM (Universal Transfer Mercator)

VI (Vegetation Index)

WGS84 (World Global reference System)

Chapter 1

1. Introduction

Global warming has immediate and recognizable effects on seasonal phenological cycles therefore; study of long term phenological series could explain how climate changes may affect the environment (Karlsen et al. 2007). In this regard, phenology parameters can be considered at both short and long time scales. While short-term climate fluctuations (e.g., temperature and rainfall) and/or human influences (e.g. extraction of ground water, urban development) may affect the annual variation of phenology parameters, long-term climate change and large scale human disturbances may cause shifts in general phenology patterns (Bradley et al. 2007). Moreover, changes in phenology may be due to changes in vegetation type, and give useful information about agriculture, ecosystem as well as climate (Heumann et al, 2007).

Maignan et al. (2008) defined vegetation phenology as "studying the time of different stages of vegetation seasonal cycle (such as leaf unfolding, flower first bloom, leaf fall…) in relation with climatic parameters." De Beurs and Henebry (2004) defined Land Surface Phenology (LSP) as discovering both temporal and spatial growing of the land surface vegetation through satellite sensors. Cyclic nature of vegetation phenology parameters, in addition to their immediate response to climate change can describe the variation of LSP.

Phenology or seasonality of vegetation can be identified from several parameters such as: the start of the growing season (SOS), end of the growing season (EOS), amplitude of the season (AMP), and length of the growing season (LOS). While the life cycle events of vegetation like bud burst, flowering, and leaf senescence cannot be directly extracted from high temporal resolution satellite sensors, they can be described and estimated by phenology parameters.

Phenology parameters are commonly extracted from vegetation indices, and among several vegetation indices, the Normalized Difference Vegetation Index (NDVI) is a widely used index for this purpose (Heumann et al .2007). Time series of NDVI can be used to observe regional and global land cover, and to analyze the global cycles of energy and matter in order to get information

about shifts in spatial distribution of bioclimatic zones as well as to extract the phenology parameters (Jönsson and Eklundh 2002).

Long-term NDVI time series is required to analyze the vegetation phenology. For that purpose, data from AVHRR (Advanced Very High Resolution Radiometer) sensors which have been archived since 1981 are commonly used in vegetation analysis. Nevertheless, the datasets suffer from quality deficiencies due to instrumentation problems, changes in sensor angle, atmospheric conditions (e.g., clouds and haze), and ground conditions (e.g., snow cover), as has been reported by Bradley et al. (2007). They argued that the identification of phenology parameters via NDVI datasets is problematic. To overcome these problems, maximum value compositing (MVC), the best index slope extraction (BISE) and spatial and temporal smoothing methods have been introduced (Bradley et al. 2007). Among different datasets based on AVHRR, data from the NASA Global Inventory Monitoring and Modeling Systems (GIMMS) group at the Laboratory for Terrestrial Physics (Tucker et al. 2005) is the most known dataset (De beurs and Henebry 2010, Fensholt et al. 2009) . Moreover, due to enhanced and high quality of dataset which was achieved from applying several correction methods (Tucker et al. 2005), this dataset is widely used.

Although several methods (smoothing functions, fitted models, thresholds and derivatives) have been studied for extracting the phenological parameters, only few methods have been developed for that purpose (Jönsson and Eklundh 2004). The TIMESAT software package as an automated method uses a model fit approach which has been developed by Jönsson and Eklundh (2002). It also has capability of merging multiple local functions, and includes the Savitzky-Golay filtering, asymmetrical Gaussian, or double logistic for large flexibility. TIMESAT has been programmed in a way that fitted function can follow the complex behavior of time series functions (Jönsson and Eklundh 2002, Jönsson and Eklundh 2004). Furthermore TIMESAT has ability to fit curves on upper envelope of NDVI time series. This capability can reduce noise related errors and soil background reflectance in NDVI, since most of errors are negatively biased (Eklundh et al., 2009).

Through applying linear regression models on time series of phenology parameters, rates of vegetation changes over a time period is observed (Heumann et al., 2007). Changes in seasonality parameters may point out variation in vegetation types and deliver information related to agriculture and ecosystems (Heumann et al., 2007). Furthermore, estimating vegetation changes

has enriched our understanding of intra and inter–annual fluctuations of vegetation changes from local to global scales (Fensholt et al., 2009).

However, linear regression may have some weaknesses regarding vegetation studies, because the changes of vegetation are not always linear. Also in some circumstances, significant abrupt changes might be overlooked by ordinary linear regression (Jamali et al., 2014); such abrupt changes may reflect environmental events such as fire, drought and land use changes. Therefore, an analysis of higher order polynomial trends could give better understanding of vegetation behavior change. Also, there may be some areas with no significant linear change, but containing notable hidden fluctuations best captured by quadratic or cubic models. These kinds of trends are named as "hidden or concealed trends" in this work. Hidden trends must be considered, since they may indicate particular events such as droughts. They can also detect when optimal fluctuations of the phenology parameters occur.

There are several factors influencing vegetation phenology such as soil moisture, rainfall, land cover and soil texture. Studying the correlation between these factors and vegetation parameter changes is required to evaluate observed changes in phenology in order to understand how they influence such vegetation changes. For instance, each land cover has different response to climate change (De Jong et al. 2012) .Therefore they can be used as reliable indicators to explain vegetation changes. Also soil moisture is identified as a better indicator than rainfall for describing vegetation greenness (Huber et al., 2011). Consequently, studying soil moisture trends helps to understand the variations of vegetation greenness.

1.1. Objective of the thesis

In this thesis, changes of vegetation phenology were investigated over the Sahelian to Equatorial area in Africa from 1983-2005 using NDVI time series of remotely sensed data. Main hypotheses of the thesis are:

1- Notable proportions of changes in phenology parameters can be described by polynomial trends.

2- Variations in phenology parameters are significantly correlated with soil moisture.

The overall aim of this thesis was to study vegetation changes through analysis of phenology parameters in the Sahelian to Equatorial area, and also to investigate increased precision when determining trends in phenology parameters using polynomial regression, rather than linear regression, for describing phenology parameters of vegetation.

Some more specific objectives that were considered are:

- Analysis of the spatial and temporal vegetation changes over the Sahelian region by applying linear, quadratic and cubic regression models to phenology parameters.

- Analysis of the variations of phenology parameters in order to detect hidden changes in vegetation dynamics (at time scales less than the length of the AVHRR record).

- Evaluation of the relationship between the phenology parameters and soil moisture as a main factor that influences the variation in phenology parameters.

- Identifying driving forces behind changes in phenology parameters, including land cover, soil texture and rainfall over the study area.

1.2. Background and theory

1.2.1. Remote sensing and the theory of its application in vegetation study

After introducing satellite remote sensing in recent decades, several studies have been done to investigate vegetation phenology using remote sensing satellite imagery. The coarse spatial resolution of high temporal data from National Oceanic and Atmospheric Administration (NOAA)/AVHRR sensor was studied by Justice et al. (1985), in order to monitor seasonal dynamic of vegetation. They found that coarse-resolution satellite data could be used as a reliable tool in order to mapping and monitoring the vegetation at regional and global scales. Jönsson and Eklundh, (2002) fitted nonlinear asymmetric Gaussian model functions to the time-series of AVHRR NDVI. They introduced TIMESAT software package to extract the phenology parameters while applied AVHRR ancillary data of cloudy days to estimate uncertainty in the data values. Zhang et al. (2003) fitted series of piecewise logistic functions to remotely sensed Vegetation Index (VI) data from Moderate Resolution Imaging Spectro-radiometer (MODIS) to show intra-annual vegetation dynamics over a large area in the United States. Results of the method coincided with behavior of the vegetation both geographically and ecologically (Zhang et al. 2003). The GIMMS AVHRR NDVI dataset was used to investigate vegetation changes over the Sahelian countries by analyzing linear trends for the time period of 1982-2005 (Heumann et al. 2007).

To study the climate change effects, the vegetation phenological data are required at large spatio-temporal scales. Since only few ground based stations have recently been established, generating data from these stations to cover a large area is challenging (Delbart et al. 2005). Satellite sensors can detect different response of vegetation to electromagnetic wavelengths (Norman et al. 2004). This property in addition to available short to long term observations of remotely sensed data has provided an opportunity to distinguish not only the vegetation types, but also the phenological changes of vegetation.

There is a specific reflectance curve for each material on the Earth surface which shows the fraction of incident radiation as a function of wavelength (Norman et al. 2004). Orientation and structure of leaf canopy including leaf pigmentation, leaf thickness, cell structure and amount of water in the leaf tissue determine reflectance characteristics of vegetation (Norman et al. 2004). Figure (1) shows an ideal reflectance curve of healthy vegetation. It is shown that, low reflectance

have been measured due to absorption in visible bands, while relatively high reflectance has been detected from near infrared band (Norman et al. 2004).

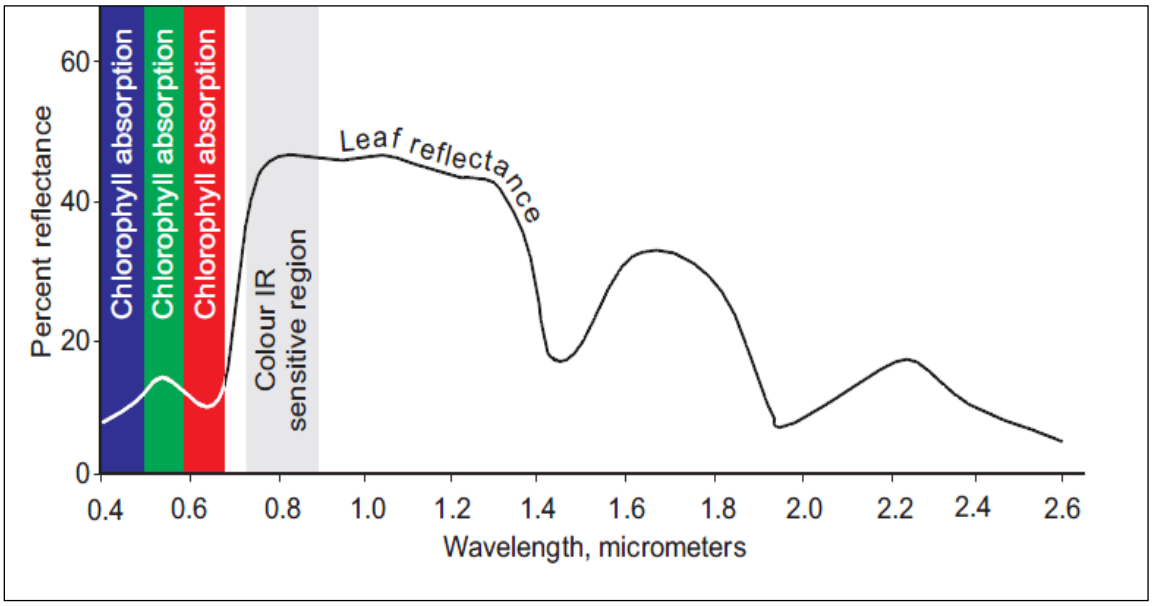

Fig.1.An idealized spectral reflectance curve of healthy vegetation (Norman et al. 2004)

As shown in the Fig. 1, there is a significant difference between red and near infrared wavelengths of vegetation where infra-red reflectance value is higher than red reflectance. Thanks to this property, vegetation indices are identified from the ratio between the values of red and near infrared bands. Among the vegetation indices, NDVI, which responds to chlorophyll abundance, is related to photosynthetic capacity and vegetation amount (Myneni et al. 1995), and is widely used to monitor vegetation (Jeong et al. 2011). NDVI is calculated based on measured spectral reflectance (Rouse et al. 1974) as:

$$\text{NDVI}=\frac{R_{NIR}-\text{R}_{red}}{R_{NIR}+\text{R}_{red}} \quad \text{Equation (1)}$$

Where: R_{NIR} is reflectance in the near infrared band and R_{red} is reflectance in the red band. From the above equation the NDVI values range from -1 to 1. NDVI illustrates the presence, density and condition of vegetation. It is related to absorb photosynthetically active radiation (APAR) and vegetation gross primary production (GPP) (Herrmann et al. 2005).

Apart from the target's spectral response, the atmosphere has significant effects on the perceived reflectance of materials through absorption and scattering (Tso and Mather, 2009). These effects could result in artificial NDVI seasonal cycle, particularly in areas with low NDVI values (Moulin et al. 1997). Another effect which should be taken in consideration refers to vegetation background. Montandon and Small (2008) argued that this effect could have a substantial influence on the reflectance, consequently also vegetation indices. They discussed that NDVI of bare soil is expected to be close to zero (NDVI~0.05), but the computed mean soil NDVI from 2906 samples was much larger (NDVI = 0.2) with remarkable variation (standard deviation = 0.1). Since there is sparse vegetation in the Sahel region, the NDVI signal acquired from AVHRR may be too weak to be distinguished from noise (Heumann et. al, 2007).

Phenology parameters are derived from the vegetation index (VI) values for each season. The general concept of extracting the seasonality parameters for one season from NDVI values is shown in the Fig. 2 (Jönsson and Eklundh, 2002).

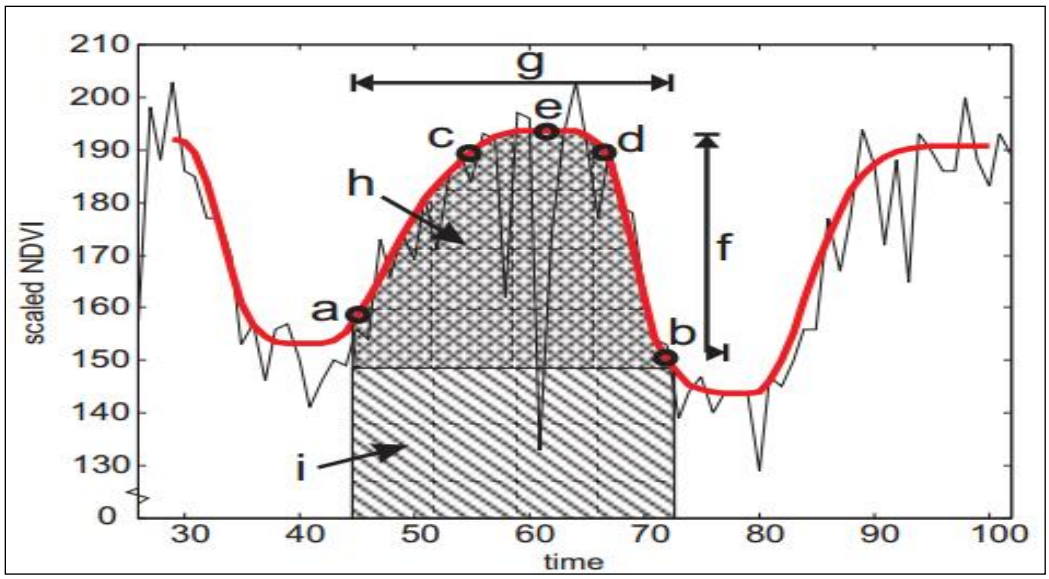

Fig.2. Schematically how the seasonality parameters are extracted from NDVI data.
Points (a) and (b) mark, respectively, start and end of the season. Points (c) and (d) give the 80 % levels. Point (e) displays the largest value. Point (f) displays the seasonal amplitude and (g) the seasonal length. Finally, (h) and (i) are integrals showing the cumulative effect of vegetation during the season (Per Jönsson and Lars Eklundh, 2002).

The procedure can be applied to several years of data through using the time series of VI. By plotting the vegetation indices against time, and then fitting a smooth curve (Red Curve) on raw NDVI data (thin black curve), the general pattern of a full season is achieved as shown in Fig.2.

1.2.2. NDVI applications in Land Surface Phenology

Phenology parameters are mostly extracted from NDVI. However this index is very sensitive and might be affected by soil color, atmospheric effects, illumination and observation geometry (Herrmann et al. 2005). However, several indices, like the Soil-Adjusted Vegetation Index(SAVI) (Huete, 1988), the Modified Soil-Adjusted Vegetation Index (MSAVI) (Qi et al., 1994), the Atmospherically Resistant Vegetation Index (ARVI) (Kaufman and Tanre,1992), and the Enhanced Vegetation Index (EVI) (Huete et al. 2002) have been introduced to offset some of these weaknesses. Nevertheless, the results did not show a consistent value for universal applications.NDVI remains as a reliable and well known index for monitoring the vegetation and it has been widely used by remote sensing researchers (Herrmann et al. 2005).

Fensholt et al. (2009) found that there is a good agreement between several different NDVI products from AVHRR sensor and in situ NDVI measurements over the semi-arid Sahelian zone for the time period of 2000-2007. They also concluded that GIMMS NDVI for annual average value trend analysis coincided well with Terra MODIS NDVI data for the semi-arid Sahelian zone, leading to a higher reliability of the results. However, they suggested caution, regarding interpretation of trends in the humid areas in Sahel due to inconsistencies between Terra MODIS and AVHRR GIMMS NDVI datasets.

1.2.3. Methods of extracting the seasonality parameters

Several approaches have been introduced and examined for retrieving vegetation seasonality parameters. The methods that have been used to extract the seasonality parameters are classified in four main categories by De beurs and Henebry (2010). These classes include smoothing functions, model fits, thresholds and derivate methods, and are discussed in this section. However, there are some limitations regarding the extraction of seasonality which could be classified in two groups:

- Limitations of datasets exist in terms of accuracy, gaps as well as overestimates or underestimates of the vegetation index. For instance, melting snow in higher latitudes leads to artificial increases of NDVI which may be indicated as an earlier SOS (Reed et al., 1994, Delbart et al., 2005). As another example, in some cases extended periods of cloudiness causes misunderstanding of the EOS (De beurs and Henebry, 2010).

- Limitations exist in terms of the methods that have been used to extract the parameters. For instance, in the case of applying a threshold, there is not a fixed threshold value to be consistent when covering a large study area (De beurs and Henebry, 2010).
Moreover, it is anticipated that there should be correlations between the parameters estimated from satellite datasets and ground based observations. While, tying satellite-based and field-based research is not easy because of two challenges: field-to-satellite scaling and selecting comparable phenological information (Fisher et al, 2006).

The phenological extraction methods have their weaknesses and strengths which influence results. For example, the curve fitting methods reduce noise and trusts on general behavior of time series data (Jönsson and Eklundh, 2002), while neglecting the spatial aggregation (Bradley et al., 2007). Also due to simplifying of smoothing functions, important phenological information may dampen and caus new errors (Fisher and Mustard, 2007).

Fitting a model on a dataset is appropriately defined in the publications relating to TIMESAT. To fit a curve on NDVI data in TIMESAT, the first step is to solve a least square model through applying required weights which could be achieved from ancillary data or STL decomposition method. “STL is a filtering procedure for decomposing a time series into trend, seasonal, and remainder components. (Jönsson and Eklundh, 2009) ”. From the first step, initial parameters of the function will be determined, afterward the NDVI values below the first fitted function are considered to be less important. In the next step the equation is solved with assigning new weights based on the first step. This process can be repeated twice in TIMESAT (Jönsson and Eklundh, 2009, TIMESAT Manual page 14). Finally, seasonality parameters of the time of the start and end of the season, the largest NDVI value, and the amplitude are computed “for each of the full seasons in the time-series (Jönsson and Eklundh, 2009).

Apart from the above capability of TIMESAT, it has several more advantages that makes it a powerful software package for extracting phenology parameters, such as: its graphical interface for viewing binary images, the possibility to define a cutoff for off-season data error management ,and a user interface. Moreover, it is a widely used software package not only for computing phenological metrics from vegetation datasets, but also for other purposes in several tasks, such as detection of forest disturbances, and testing eddy covariance data and moisture data (Eklundh et al. 2009). For more information refer to: (http://www.nateko.lu.se/timesat/)

The four extraction methods in addition to an overview of their benefits and drawbacks are described in the following sections. The first two methods describe the general pattern of data, while the last two methods are concerned with the extraction of the parameters after fitting a model.

A) Smoothing functions

This category consists of several sub-methods which use a smoothing function to describe the dataset changes over time, and define the parameters based on a smoothed function.

Reed et al. (1994) defined the SOS and EOS as dates where the smoothed time series line passed the curve of a moving average model. Since it is assumed that the phenology is well represented by a moving average model, the method may not be applicable for data with disturbances and land surface changes (De beurs and Henebry, 2010, page 186). The method is also not appropriate in areas with rapid response to precipitation (De beurs and Henebry, 2010). The Savitzky-Golay method was implemented by Jönsson and Eklundh (2004) based on least square fit to upper envelop of the NDVI data, using local polynomial functions. In this method, a moving average window is selected, and each data value is replaced with a linear combination of nearby values. The method uses a local function, it is appropriate to be applied on data with less noise (Jönsson and Eklundh, 2004). Positive point about this method is that the method can track complex behavior of data.

Olsson and Eklundh (1994) and Moody and Johnson (2001) examined the discrete Fourier analysis approach, using a sum of sinusoidal waves at several frequencies to estimate the curve. They found that the approach responds well to systematic changes, but is comparatively unresponsive to

nonsystematic data noise. After ignoring higher order harmonics, it is possible to retrieve lower signals of noise which performance basic behavior of the vegetated surface (Moody and Johnson, 2001).The first harmonic conveys mean NDVI and overall productivity of a region, and its amplitude illustrates changes in the productivity over the year (Moody and Johnson, 2001). In a case of very regular cyclic temporal patterns, results of this approach could successfully show ecological behavior of a region, while there are limitations when applying the approach to an area with unrecognized ecological behavior (Moody and Johnson, 2001).

B) Model Fit

In this method, a model is fitted to the dataset, and phenology parameters are extracted based on the fitted curves and threshold or derivate methods. Several models have been developed in order to fit curves to time series of vegetation indices. The first model was a parameterization of an NDVI temporal profile (Badhwar 1984). Zhang et al. (2004) fitted a logistic model to Enhanced Vegetation Index (EVI) in two separate parts: vegetation growth and senescence; then the SOS and EOS were extracted based on the derivative of curvature function on both parts.

Asymmetric Gaussians and double logistic functions were fitted to data as local models (Jönsson and Eklundh 2002, 2004). The functions are well matched for describing the time series around optimum points while they are not well suited at the limbs. Therefor the local model functions are merged to a global function. Advantages of these models are the flexibility of the fittings, allowing the functions to follow complex behavior of the time series (Jönsson and Eklundh 2002, 2004).They finally defined SOS and EOS from a global model using the threshold method.

C) Threshold

In this category, the SOS and EOS can be derived from an absolute threshold (when the NDVI crosses a certain value) or a relative threshold (e.g. when the NDVI passes the certain percentage of the seasonal amplitude). Since different areas do not have the same phenology cycles, particularly when latitude changes, a fixed threshold value may not properly observe phenological events and results will not be reliable (De beurs and Henebry, 2010).

Karlsen et al. (2006, 2007) applied a threshold to select SOS and EOS for 21 years-mean vegetation values. By defining a baseline year, Shabanov et al. (2002) selected the NDVI of 120

Day Of Year (DOY), and 270 DOY of median year as the threshold values to find SOS and EOS. White et al. (1997) defined the NDVI ratio as:

$$\text{NDVI ratio} = \frac{\text{NDVI} - \text{NDVI}_{min}}{NDVI_{max} - \text{NDVI}_{min}} \quad \text{(Equation 2)}$$

Where NDVI_{min} and $NDVI_{max}$ could be defined annually (White et al., 1997), or as mean maximum and minimum of the long-term NDVI (Kogan, 1995). They determined SOS and EOS as dates when NDVI ratio passed 50% in upward and downward directions, respectively. Delbart et al. (2005) introduced a threshold based method for the Normalized Difference Water Index (NDWI) for areas with snowfall. NDWI, which responds to water content of vegetation, has been used as an index to observe the stress of water in semi-arid areas, map burnt areas in boreal forests, as well as describing land cover and vegetation types (Delbart et al, 2005). They discussed that SOS in such areas results from snow melt rather than vegetation greenness. Although the method can separate green-up from snow melt; there are some limitations for applying the method because of lack of a fixed threshold value that could be found for all land cover types (Delbart et al, 2005).

D) Derivative

The derivative methods assign the time of greatest increase and decrease in NDVI as SOS and EOS, respectively (De beurs and Henebry, 2010). SOS was defined as the time of the greatest positive derivate due to occurring fast and rapid increasing of NDVI, while EOS was determined as the time of the lowest negative derivate due to rapid decrease in NDVI (Tateishi and Ebata, 2004). Baltzer et al. (2007) applied 5 composites moving window which passed over every pixel of the time series. They calculated regression slope of NDVI against time for every window, then the second ordered derivate was calculated for the same moving window. They assigned SOS as a day that the second derivate of the moving window regression reached the local maximum of 13-composites window with a positive slope. EOS was calculated in the same way but with a negative slope. Use of the method was based on the assumption that SOS and EOS occur at a breakpoint in the time series, while in some environments this may not be the case.

1.2.4. Trend Study

Vegetation changes affect phenology parameters. Therefore, investigating the trend of phenology parameters can describe vegetation changes. De Jong et al. (2012) defined the trend as the direction and rate of change through time, which usually is derived from the slope of a linear regression model.

Several studies applied the trend analysis for investigating vegetation changes. Eklundh and Olsson (2003) studied trends in vegetation greenness for African Sahel from 1982-1999, they found "a strong increase in seasonal NDVI over a large area". Through studying the vegetation trend in Sahel, Olsson et al. (2005) found that "increase rainfall is a certain reason, while other factors, such as land use change and migration, may also contribute". Seaquist et al. (2009) tested the effects of climate and people on vegetation dynamics in Sahel, while they did not find a significant human footprint on vegetation dynamics.

The trend results of three different NDVI dataset (Pathfinder, GIMMS and FASIR), which have been produced from AVHRR data were compared by McCloy et al. (2005). All three datasets indicated an increasing average global trend, while some variations from one dataset to another were recorded (McCloy et al., 2005).

The BFAST (Breaks For Additive Season and Trend) package was published in 2010 by Jan Verbesselt and his colleagues as a part of R programing language (Verbesselt et al., 2010). The package is used to decompose time series into trend, seasonal, and remainder components. The method is also used to detect and describe abrupt changes within a trend and seasonal components (Verbesselt et al., 2010). De Jong et al. (2012) used the BFAST method to detect and describe the breaks in the trend components over the world by using GIMMS NDVI time series from 1981 to 2008.

Most of the vegetation trend studies have been concerned with analyzing linear trends in NDVI, and there are only few studies that examined the trend of phenology parameters. An example of the latter is Heumann et al., (2007) who analyzed TIMESAT derived phenology parameters in Sahel, Soudan and Guinean regions using 10 day MVC of GIMMS NDVI dataset from 1982 to 2005. They used ordinary least squares trends within 95 % of significant interval to analyze the

phenology parameter changes. Due to high probability of noise, Heumann et al. (2007) defined a 20% threshold for estimating SOS and EOS, in addition to excluding the data values less than 0.1 NDVI units.

Jamali et al. (2014) applied an automated method for analysis of non-linear vegetation changes. They argued that linear trends cannot fully represent vegetation changes, and some information will be ignored. They also mentioned that vegetation changes do not always have gradual and constant changes. Several classes have been distinguished in their study: linear, quadratic, cubic, hidden, and no-trend classes. These polynomial trends can give indirect explanation of vegetation change occurrence on a case-by-case basis (Jamali et al., 2014).
Note: In this thesis the algorithm of Jamali et al. (2014) and some parts of their scripts were used to analysis the parameters.

1.3. Data

1.3.1. GIMMS NDVI dataset

The GIMMS NDVI dataset (Tucker et al. 2005), which is a bimonthly composite of NDVI with a spatial resolution of approximately 8 km, was used to estimate and investigate the phenology parameters from January 1983 to December 2005. Low NDVI values are affected by soil background reflectance more than high NDVI values; therefore, low NDVI may relate to false vegetation values (Tucker et al. 2005). However, after applying Empirical Mode Decomposition (EMD) and Maximum Value Composition (MVC) methods, these effects were limited (Tucker et al. 2005). The MVC has been applied to the GIMMS dataset by assigning the maximum NDVI value to pixels during 15 days of regularly spaced interval in order to reduce the cloud cover effects (Tucker et al. 2005).
Chappell et al. (2001) pointed out that due to structure of the surface and the atmospheric scattering, radiation on the surface would be not equal in different direction (anisotropy). They also argued that implementation of MVC algorithm without considering the anisotropy may results in a large NDVI values because of directional effects rather than atmospheric effects. To minimize these preferential errors, GIMMS NDVI dataset has been corrected from:
- Residual sensor degradation and sensor inter-calibration differences

- Effects of changing solar zenith and viewing angles due to satellite drift
- Volcanic aerosols
- Distortions caused by persistent cloud cover globally
- Low signal to noise ratios due to sub-pixel cloud contamination and water vapor (Tucker et al. 2005).

Another error that may occur refers to transitions between the platforms which may cause discontinuity of data, but the error is not anticipated to affect the trend slope (De Jong et al., 2012). Volcanic eruptions can be seen over dense vegetated tropical land covers for limited time periods causing NDVI signal reduction (Tucker et al. 2005). The dataset has also been validated through comparing with the well-calibrated and atmospherically-corrected MODIS dataset for the period of 2000-2007 over the semi-arid regions of the Earth (Fensholt et al., 2012).

1.3.2. Modeled soil moisture dataset

A monthly soil moisture dataset, which has been created by the Climate Prediction Center (CPC) placed in National Oceanic and Atmospheric Administration (NOAA) agency, is available from the time period of 1982 to 2008, and was used in this work. The soil moisture model was produced based on the equation (3)

$$\frac{dw}{dt} = P\text{-}E\text{-}R \quad \text{equation (3)}$$

Where, w stands for soil moisture and P, E and R are precipitation, evapotranspiration and runoff, respectively (Fan and Dool, 2004). They used Climate Prediction Center (CPC) monthly global precipitation over land, which was covered by over than 17,000 gauges worldwide, and monthly global temperatures from the CDAS- Re-analysis product, as driving input fields in the model . Outputs of the model consist of global monthly soil moisture, evaporation and runoff (Fan and Dool, 2004). They also validated the model with in situ observations around the world. Results showed that simulation was reliable compare to measurements of seasonal to inter-annual variation of soil moisture in many places of the world (Fan and Dool, 2004). Theunit of the result is mm in a single column of 1.6 meter, and maximum value is set to be 760 mm in the model. Since spatial resolution of the dataset was 0.5 degree, they were resampled to 0.0727 º degree of spatial resolution and projected to UTM WGS84 geodetic reference system.

1.3.3. Land Cover data

The Global Vegetation Monitoring unit belongs to the research Center of European Commission coordinated implemented the Global Land Cover 2000 Project (GLC 2000) in cooperation with some other partners around the world. They used a 14 months dataset of preprocessed daily global data, using the vegetation sensor on board the SPOT 4 satellite to accomplish the project. They also used the FAO Land Cover Classification System (LCCS), and allowed the partners to describe their regional land cover classes, and define their legends in addition to following a standard classification approach. They used global classes to show the vegetation types and density of the cover, independent from climate zones. The land cover of Africa, including 27 main classes, was clipped to the study area and defined within the WGS84 spatial reference. Afterward the data was resampled from one kilometer to 8 kilometer spatial resolution as shown in Fig.3.

For more information about GLC 2000 Land cover data or for downloading the product, go to: (http://bioval.jrc.ec.europa.eu/products/glc2000/glc2000.php).

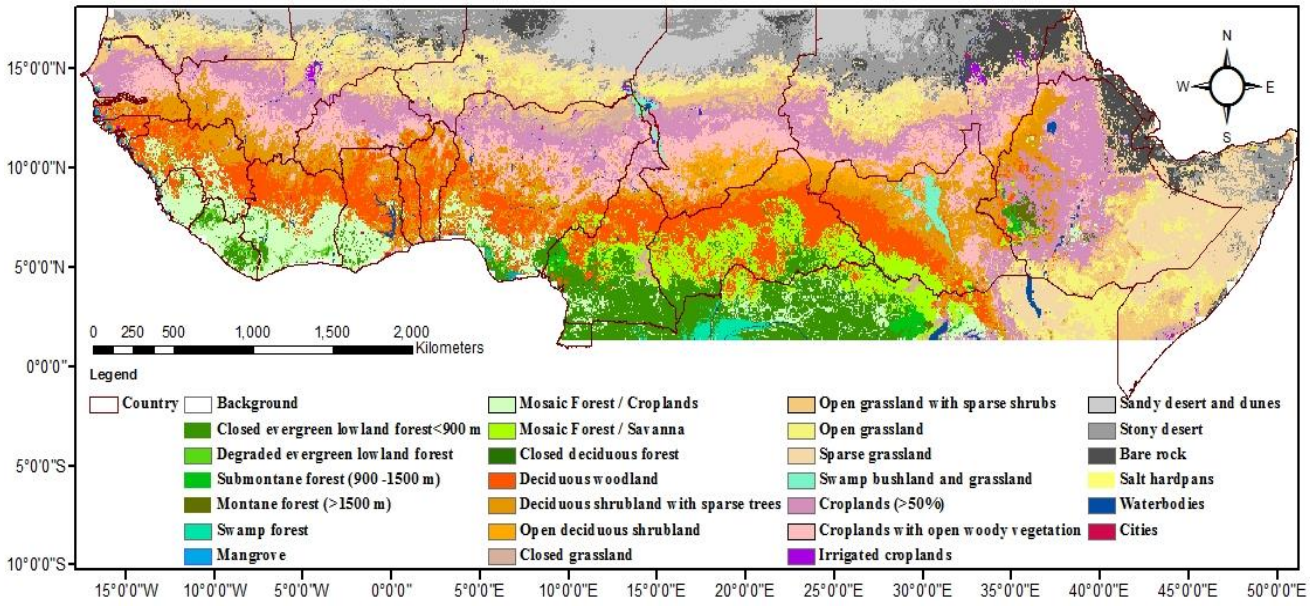

Fig.3. Land Cover Map of 2000 over the study area (GLC 2000)**.**

1.3.4. Soil Map data

The global Soil region map was digitized by ESRI (Environmental Systems Research Institute) is based on a reclassification of the FAO-UNESCO Soil Map of the world combined with a soil climate map. The soil map data produced in April, 1977 and revised in September, 2005 covers the

globe in a minimum scale of 1:5,000,000. The global soil map was resampled from about 4 km to 8km spatial resolution

(http://soils.usda.gov/use/worldsoils/mapindex/order.html).

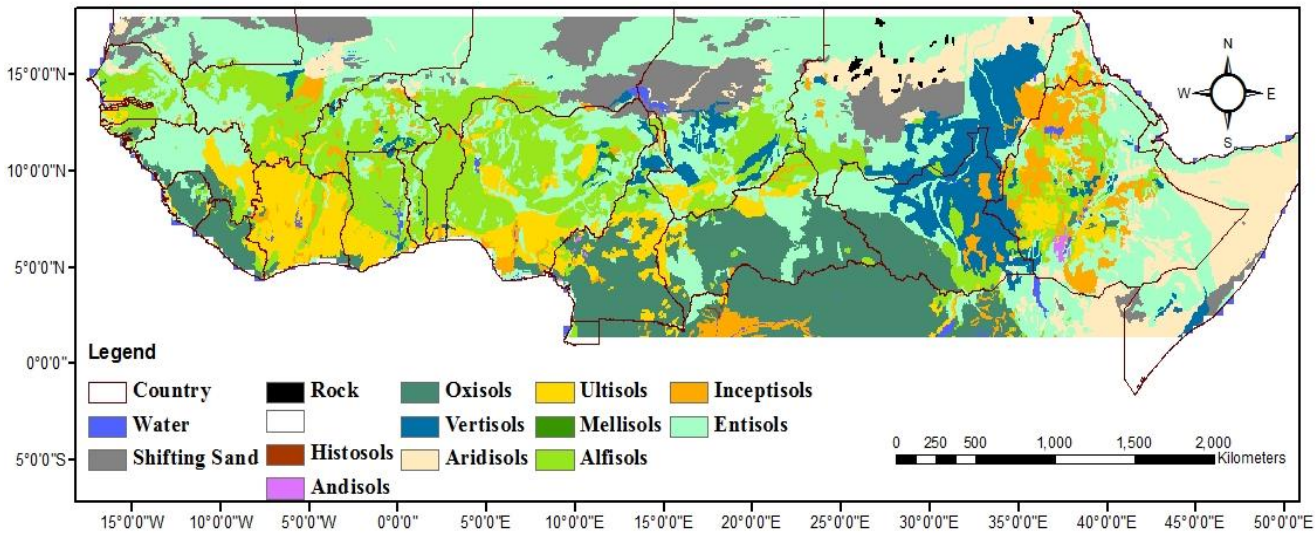

Fig.4. Soil Texture Map over the study area. Source: FAO-UNESCO.

The study area was clipped and defined using the WGS84 geodetic spatial reference system. In this project the original soil map was reclassified into 12 main classes based on FAO-UNESCO classification, as shown in Fig.4 and Table.1.Table.1illustrates the main soil map classes regarding to their locations and characterizations according to NRCS (Natural Resources Conversation Service), and also their percentages in the study area. As shown, Entisols, Alfisols, Oxisols, Aridisols, Ultisols, Vertisols and Inceptisols are the main soil texture types that cover the study area. Around 8% of the study area is covered by other land types: shifting sand, 6.8%, water bodies, 1%, and rock, 0.2%.

Table 1. 12 Soil texture types with their characterizations and their percentage over the study area, based on FAO-UNESCO classification, NRCS.

Soil order	Location	Description
Entisols	Occur in many environments	Characterized by absence of pedogenic horizon development and likely to found in flood plains, dunes and steep slopes.

Alfisols	Semiarid to moist areas	Characterized by holding water and nutrients to plants, occurs under high dense vegetation regions like as forest or mixed vegetation cover and it's a good productive soil for crops.
Oxisols	Tropical and Subtropical regions	Characterized by low fertility and a low capacity to retain additions of lime and fertilizer.
Aridisols	Deserts of the world	Highly dry soil for the growth of plants, characterized by lack of moisture and accumulating gypsum, and salt.
Ultisols	Humid areas	Nutrients are concentrated in the upper zone of soil, and it is classified as acid soils that can't retain addition fertilizer and lime easily.
Vertisols	Occur in many environments	Characterized by high content of expanding clay minerals that transmit water very slowly and tend to be high in natural fertility.
Inceptisols	Semiarid to humid environments	Characterized by a moderate degree of soil weathering and development in a wide variety of climates. .

1.3.5. Annual Rainfall

The average annual rainfall map of Africa over a period of 1951-1980 was published by UNEP in 1992 as results of a cooperative effort between UNEP's Desertification Control Program Activity Centre (DC/PAC), the Global Environment Monitoring System (GEMS) and the Global Resource Information Database (GRID).

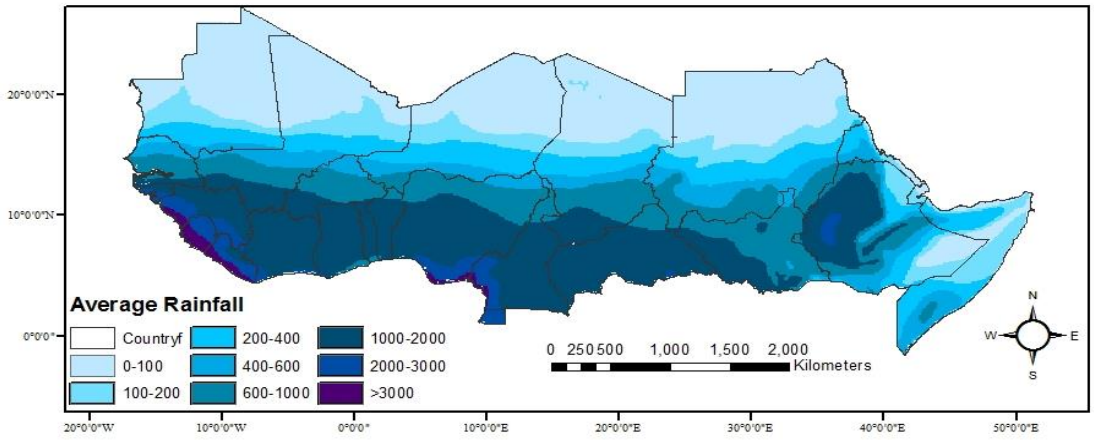

Fig.5. Mean annual rainfall over the Sahel, UNEP 1992

The mean annual rainfall is based on precipitation and temperature stations data from UEA/CRU for two 30-year periods, 1930-59 and 1960-89. The rainfall data was in shape file format, and is defined in the WGS 84 geographic system. The data were clipped to the study area and classified

to 8 main classes as shown in Fig.5. For more information please go to: (http://ede.grid.unep.ch/mod_download).

1.4. Study area (definition and characterization)

The area between the arid Sahara in North Africa and the humid tropical savanna in the Equatorial area was selected to be analyzed in this thesis. Due to substantial variation in rainfall during the recent decades (Heumann et al. 2007), and being a transition area, it has been studied intensively in order to detect, understand and monitor vegetation changes.

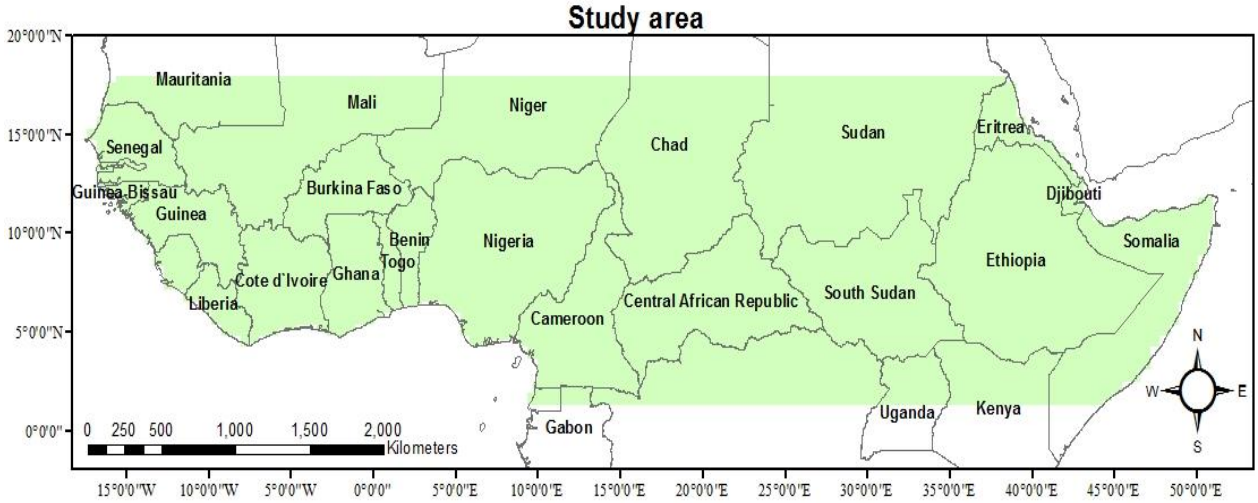

Fig.6. The study area, green color from 1.324˚ N to 19.36036296˚N & 19.127˚W to 52.94572457˚E where North and South Atlantic oceans, Arabian Sea, Red Sea, Islands in African coasts and Yemen were excluded.

The area includes four sub eco-climatic zones including the Sahelian zone, the Sudano-Sahelian zone, the Sudanian zone and the Guinean zone (Fig. 7). These zones were introduced based on the average annual precipitation and agriculture features (FAO/GIEWS, 1998) as shown in Fig.7. The Sahelian zone is a region with average annual rainfall between 250 and 500 mm, and scant permanent vegetation. Only pastures and short-cycle cereal crops which are resistant to drought exist in the area. All crops in this zone are highly vulnerable. The Sudano-Sahelian zone is a region with average annual rainfall between 500 to 900 mm. Sorghum and millet with a short growing cycle of 90 days are the main cultivated crops growing in this area. The Sudanian zone is a region with average annual rainfall from 900 to 1100 mm. Maize, root and cash crops with a growing

cycle of 120 days or more are dominant crops growing in this area. The Guinean zone is a region with average annual rainfall more than 1100 mm. Root crops are more suitable in the Guinea-Bissau and a small area of southern Burkina Faso (FAO/GIEWS, 1998).

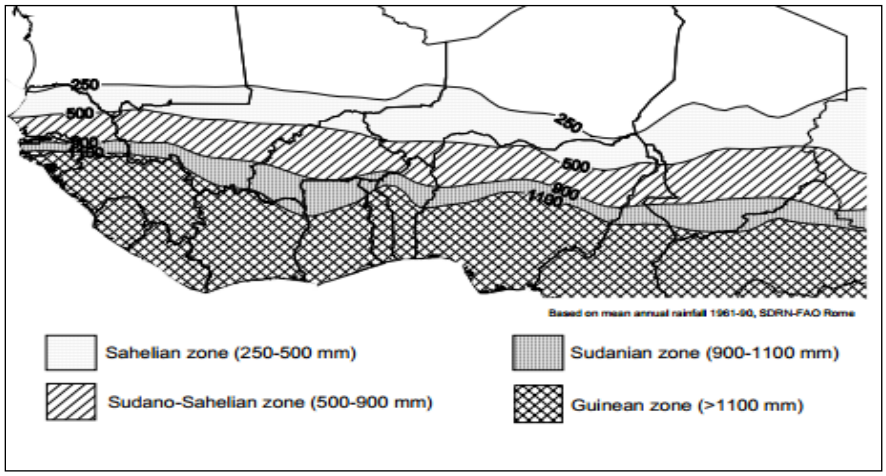

Fig.7. Four eco-climatic zones in Sahel:
Sahelian
Sudano- Sahelian
Sudanian
Guinean
(FAO/GIEWS, 1998)

Intensify of vegetation amount decreases from south toward north, from savanna forest and cropland in the south to stony and sandy desert in the north of the region as shown in Fig.3. While the southern part of study area is dominantly covered by evergreen forest, east part including north of Kenya, Somalia, Eritrea, and Djibouti and east part of Ethiopia are covered with sparse grassland and classified as dry climate.

Some exogenous rivers in the area play an important role in agriculture and livestock industry including the Senegal, Niger, Volta and Nile rivers (Le Houerou, 1980). The wells have the small quantity of discharge, and deep ground water rarely exists in the region (Le Houerou, 1980).

In this area, the mean annual rainfall follows a north to south gradient (Fensholt et al., 2009). Rainfall which occurs from mid-June to mid-September (Le Houerou, 1980) has had decadal fluctuation and large inter-annual variability (Huber et al., 2011). Nicholson (2005) found that this variability is mostly related to the August rainfalls as the wettest month in the Sahel because of the remarkable contribution of August rainfall to inter-annual variability.

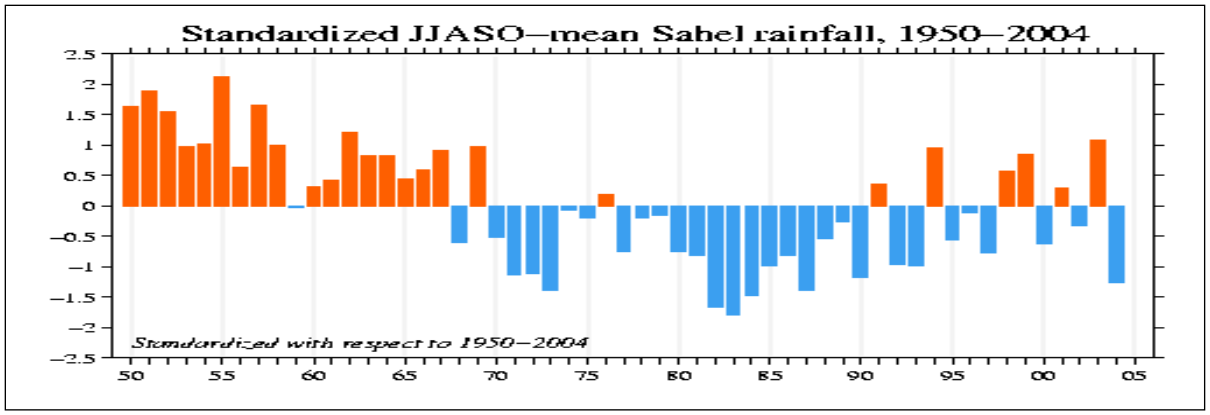

Fig.8. June through October averages of the Sahel rainfall series, http://www.jisao.washington.edu

Fig.8 illustrates mean rainfall for the Sahel for JJASO period (July, June, August, September and October) which has been standardized for the period of 1950 to 2004, in a way that the mean and standard deviation of the series became 1 and 0, respectively. A significant decrease in mean rainfall is seen from 1970 to 1990, while after that period the mean rainfall has been fluctuating.

The temperature has an average maximum from 40-42˚C in April-May to average minimum of 15˚C in December-January in the Sahel region; the potential of evapotranspiration is very high and the air humidity is extremely low (Le Houerou, 1980).

While some research (Mitchell and Hulme, 1999; Held et al., 2005) pointed toward a drier climate for Sahel in the next 50-100 years, there were some others (Haarsma et al., 2005) that expect a wetter Sahel with a seasonal precipitation increase up to 30%. Although The IPCC Third Assessment Report (TAR) had challenged the results of increasing the greenness over Sahel (IPCC, 2001), regarding the vegetation in Sahel, recent remotely sensed studies (Rasmussen et al., 2001; Olsson et al., 2005; Herrmann et al., 2005) show an increased greenness in most parts of Sahel, which was a response of semi-arid ecosystems to variation in climate, and capacity of the area to cover from droughts (Eklundh and Olsson, 2003).

Chapter 2

2. Methodology

The GIMMS dataset was analyzed in order to examine the polynomial (quadratic, cubic, hidden quadratic and hidden cubic trends) trends of vegetation phenology over the Sahelian to Equatorial region.

Figure 9 shows the general processes of the seasonality, trend analysis and spatial comparison. In the first step, 5 main phenology parameters (SOS, EOS, LOS, AMP and Small Integral of the season (SI)) have been extracted using the TIMESAT software. Following this, the polynomial regression algorithm was applied to the phenology parameters. The ArcGIS software was used to extract more information regarding the areas with significant changes, and also to generate the required maps from the results.

Also, the polynomial regression algorithm was applied to derive polynomial trends of the modeled soil moisture for each month. Phenology trends and soil moisture trends were compared in order to find the relationship between soil moisture and each phenology parameter.

As each land cover has different response to climate change (De Jong et al. 2012), results were compared against the land cover map of the study area. Finally, since impacts of climate change on soil moisture may depend on soil texture (Bormann, 2012); soils map data was considered to interpret the results of phenology trends. Finally the mean annual rainfall as a climate driver was considered and overlaid on the results.

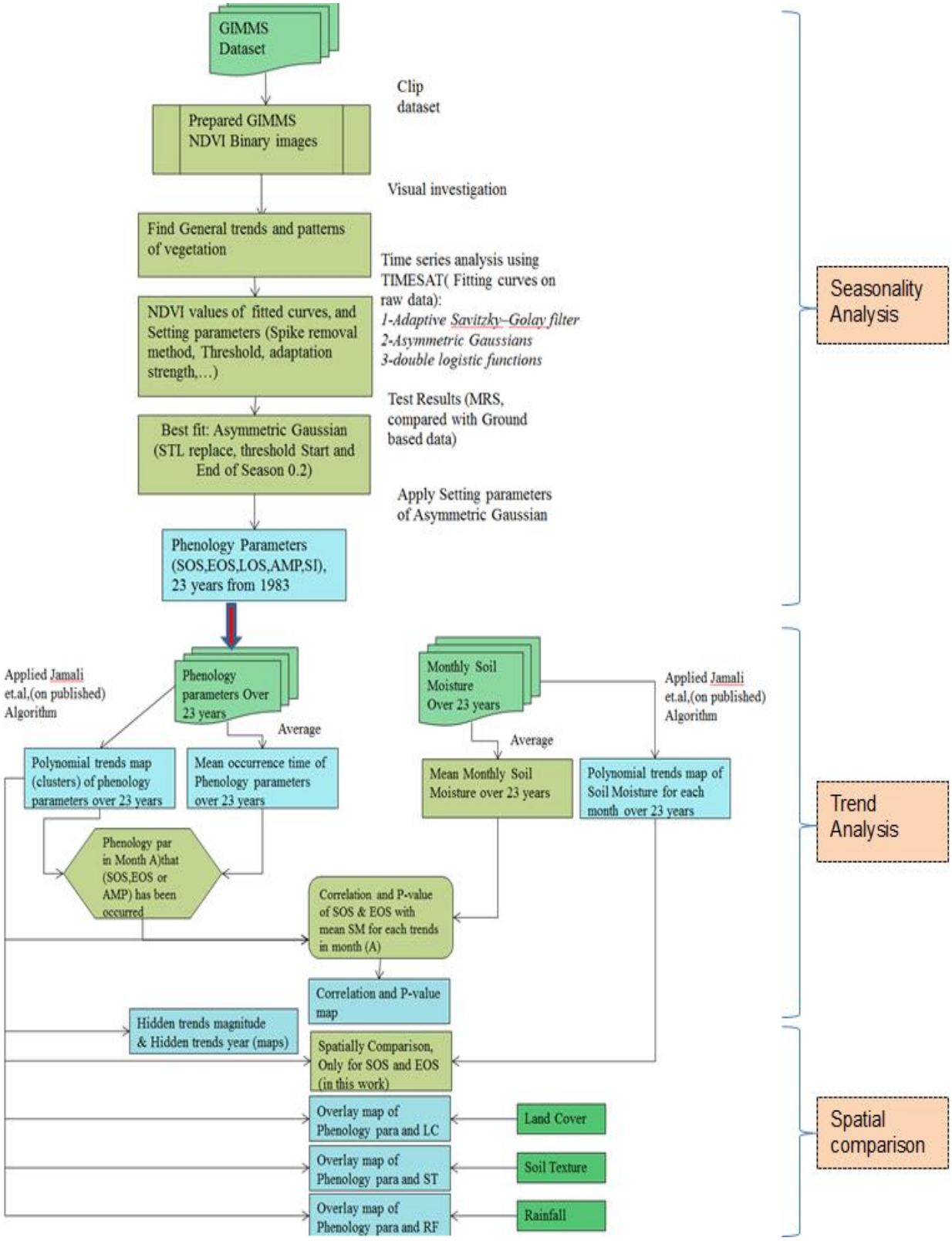

Fig.9. Description of the processes of seasonality analysis in the study.

2.1. Seasonality analysis

2.1.1. Pre-processing of data

Through using a MATLAB script, written by Lars Eklundh, the global GIMMS NDVI data was clipped to the study area domain.

2.1.2. Extracting the phenology parameters using TIMESAT

Several steps were done to extract the final phenological parameters from clipped GIMMS NDVI time series using TIMESAT.

2.1.2.1. Visual investigation of images

GIMMS NDVI binary images were visually observed in TIMESAT in order to comprehend the NDVI pattern over the study area. For instance, the general pattern indicates increasing NDVI from north to south as shown in Fig.10. The highest greenness occurred around ITCZ (Inter-Tropical Convergence Zone), extending from 10º E to 35ºE longitudes. Through investigating the NDVI data in TIMESAT, it was realized that NDVI values in some areas, particularly northern areas, were too low to be distinguished from noise. Also inter-annual changes occurred in these areas. Therefore, such areas may not show real vegetation seasons and therefor cause errors. These problems were taken into consideration during the interpretation of the results.

Fig.10 illustrates how the NDVI varied over the study area, spatially and temporally. Fig. 10A illustrates the NDVI values of MVC of first 15 days of February 1983. Figures (10B and 10C) represent the MVC NDVI values regarding the first 15 days of February 2003 and September 1983, respectively. As a general consideration the NDVI increases from North to South in the study area. Although not remarkable, NDVI changes happened from 1983 to 2003 in February, and some notable changes of NDVI were recorded from February to September, 1983. Through investigating the NDVI imagery in TIMESAT, the general trends and patterns of vegetation changes were observed.

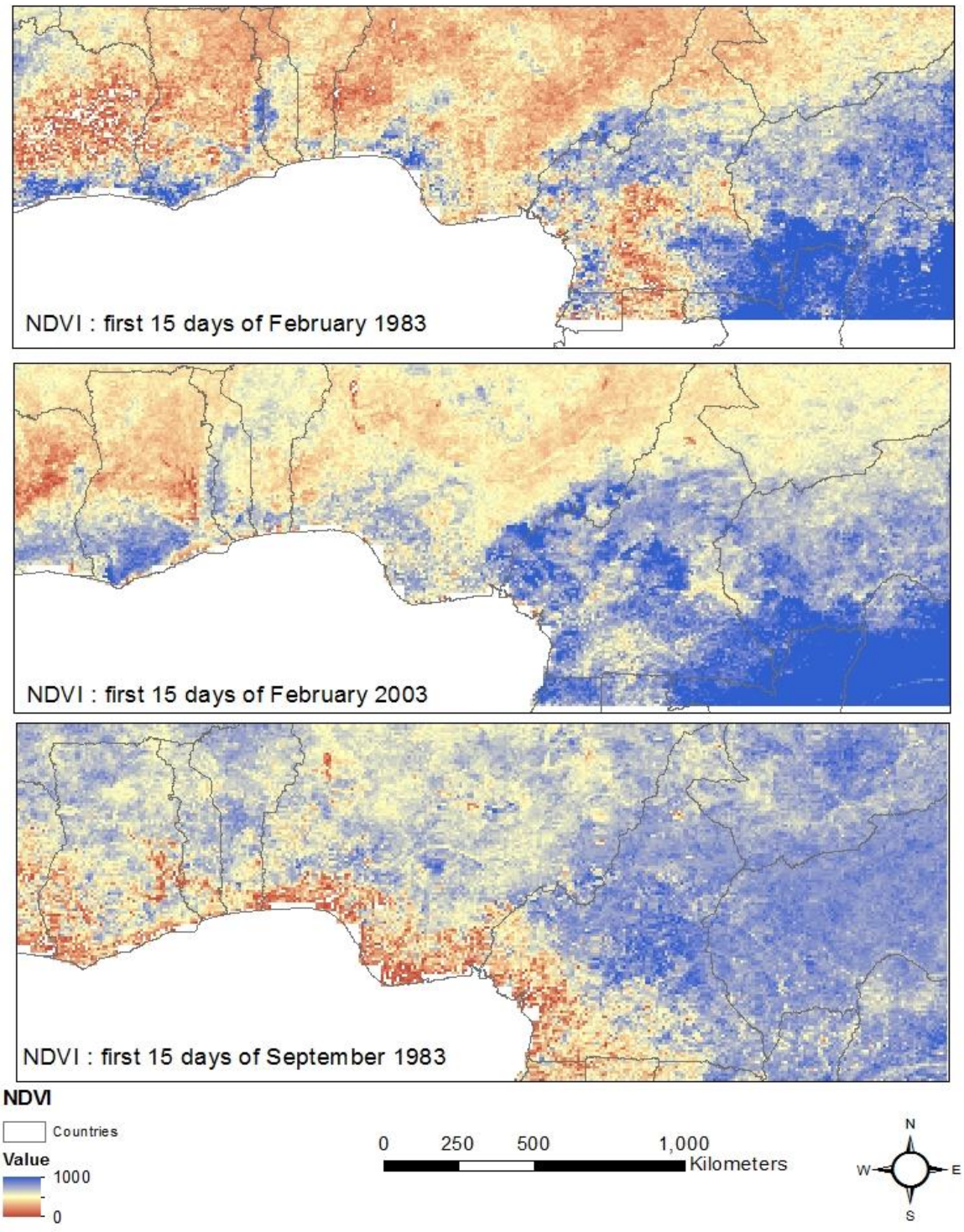

Fig.10. MVC NDVI of first 15 days of February 1983(up), February 2003(middle) and September 1983(down). NDVI values have been up-scaled to 1000.

2.1.2.2. Processes to define setting parameters

The first step in processing the data in TIMESAT was to define the setting parameters, in order to apply it to NDVI time series. Since NDVI from different land covers may follow different pattern, there is a capability in TIMESAT to define several sets of parameters based on land cover. Setting parameters define how the smoothing model or the fitted curve can represent fluctuations of the NDVI data, in addition to define extracting methods. The setting parameters are parameters related to: spikes removing methods, number of upper envelope, and the threshold value. Three methods have been developed in TIMESAT to fit a curve on data, which are based on least-square method fits to the upper envelop of the NDVI data: Savitzky-Golay, asymmetric Gaussians and double logistic functions (Jönsson and Eklundh, 2009). As shown in Table. 2, for each method of extraction setting parameters were changed to find the best fitting curve. Only relative threshold of 20% and 50% of amplitude was used to define SOS and EOS. Regarding removal of the spikes, since no ancillary data was used, only a median filter and the STL technique for replacing outliers were applied on the dataset. The strength of adaptation to the upper envelope was assigned as levels of 2 and 3.

Fitting a curve or model on dataset

1) Adaptive Savitzky–Golay filter

The savitzky-Golay filtering is a smoothing method and uses the moving window in order to replace values with a linear combination of nearby values (Jönsson and Eklundh, 2009) .In this method, the values are obtained from the quadratic polynomial least square fit function to all 2*n+1 points in the moving window (n points backward and forward). In order to overcome the negatively biased noise, the fitting process is done in several steps and will be adapted to the upper envelope of the NDVI values (Jönsson and Eklundh, 2009). The degree of smoothness in the Savitzky-Golay approach depends on the parameter of "n", and can be defined in TIMESAT. For the areas with larger fluctuation in NDVI, it is better to define smaller values for the parameter; otherwise the abrupt changes are smoothed out. In this thesis n = 4 was defined as the degree of smoothness for all the methods.

2) Asymmetric Gaussians and double logistic functions

These two methods use similar approaches with different mathematical functions. In these methods, local functions are fitted to data in the interval around the maxima and minima (Jönsson

and Eklundh, 2002). While the local functions properly describe the NDVI data in overlapping intervals around maxima and minima, the accuracy around the limbs is lower (Jönsson and Eklundh, 2002). To handle this, the local functions are fitted in several steps. Since negatively biased noise must be considered in the processes, the functions are fitted to the upper envelope of the NDVI time series data, (Jönsson and Eklundh, 2009). The merging function allows the functions to follow complex behavior of the data (Jönsson and Eklundh, 2002).

Ancillary quality data and removal of outliers

The possibility of using ancillary data as weights on the dataset has been well developed in TIMESAT (Jönsson and Eklundh, 2009). For instance, ancillary data could be used, e.g. data that describes the ratio of cloudy days in the MVC dataset of NDVI, which may vary from zero for fully cloudy to one for no clouds. Although ancillary quality data reduces most spikes and outliers, some outliers still remain, which may affect the degree of smoothness (Jönsson and Eklundh, 2009). Three different methods to remove the spikes have been introduced in TIMESAT. In the first method, the weight of data points having substantially different values from the neighbors and median values, are assigned to zero. In the second approach, the weights of data points are assigned based on the STL method (Cleveland et al. 1990). Data values that deviate from the seasonal cycle are assigned low values. In the third approach, weights are chosen based on the product of assigned STL decomposition weights and the ancillary weights (Jönsson and Eklundh, 2009).

Note: as no ancillary data was used, the first and second spike methods were applied in this project. The STL decomposition method was chosen as the final method for removing the spikes.

2.1.2.2. Extracting the seasonality parameters from the curves

A relative or absolute threshold can be applied to the NDVI time series to define SOS and EOS of each season. In the first approach SOS and EOS are determined as the date when the fitted curve crosses an absolute threshold value. In the second method, these parameters are defined as when the curve reaches a fraction of AMP, which is measured from the left or right minimum value (Jönsson and Eklundh, 2009). For this purpose, a range between 0 and 1 can be selected in TIMESAT. However, due to possible noise in data, especially in the dry season (Heumann et al, 2007), the minimum values may not represent a real value and cause errors in the results. In this thesis, only a relative threshold (of the seasonal amplitude) was determined. Since in some areas

two or more growing seasons may occur, the possibility of selecting the number of seasons has been embedded in TIMESAT (Jönsson and Eklundh, 2009). Nevertheless, only one season was assumed to occur in the study area.

Table.2 shows a summary of methods and processes which have been applied to the dataset. All parameters related to removal of outliers were applied for each of the three methods of fitting functions in TIMESAT (adaptive Savitzky–Golay filter, asymmetric Gaussians and double logistic functions (Jönsson and Eklundh, 2009).

Table 2. Summary Settings information of parameters related to three methods of extracting the seasonality parameters in TIMESAT.

Method	Spike method	Start of season method	Adaptation strength	Savitzky-Golay window size	Value for start the season	Value for end of the season
Savitzky- Golay(1)	Median filter	Amplitude	3	4	0.2	0.2
Savitzky- Golay(2)	Median filter	Amplitude	3	4	0.5	0.5
Savitzky- Golay(3)	STL replace	Amplitude	2	4	0.2	0.2
Asymmetric Gaussians(1)	Median filter	Amplitude	3		0.2	0.2
Asymmetric Gaussians(2)	Median filter	Amplitude	3		0.5	0.5
Asymmetric Gaussians(3)	STL replace	Amplitude	2		0.2	0.2
Double Logistic(1)	Median filter	Amplitude	3		0.2	0.2
Double Logistic(2)	Median filter	Amplitude	3		0.5	0.5
Double Logistic(3)	STL replace	Amplitude	2		0.2	0.2

Several ground observation stations have recently been established in the Africa, though they are not many enough to cover the area spatially and temporarily (Delbart et al. 2005). In this thesis the fitted curves values of NDVI for all different methods were compared against half-hourly in-situ

rainfall data from NE-Waf ground based station (Wankama fallow station in Niger), using MRS (Mean Root Square) method. Due to recently establishing of ground based station, only NDVI data of 2005 was used in the analysis. Finally asymmetric Gaussians function with the characteristics described as asymmetric Gaussian (3) in the Table.2 resulted in the best fits, and was selected to be the preferential method used in TIMESAT in the following processing.

2.1.3. Data Processing in TIMESAT

In this step, the best fit method was applied in the study area. It is noticed that in TIMESAT there is an ability to apply different setting parameters based on land covers or quality indicators (Jönsson and Eklundh, 2009). However, as different settings in different land use areas were not deemed necessary, only one set of parameters was applied on the whole study area.

2.1.4. Post-Processing

In this step, the phenology parameters (Start of Growing Season (SOS) ;End of Growing Season (EOS); Length of Growing Season (LOS) ; Amplitude (AMP) ; Small Integral (SI)) were generated for all 23 years (because the first and last seasons are not automatically achieved in TIMESAT), using a MATLAB script written from Lars Eklundh and Per Jönsson.

The generated annual parameters from TIMESAT were used as input for estimating polynomial trends over the whole study area. The following section describes the methods that used for investigating the phenology changes.

2.2. Trend analysis

2.2.1. Phenology Trends

The TIMESAT derived phenology parameters (SOS, EOS, LOS, AMP and SI) of 23 years were used to compute polynomial trends for the time period of 1983-2005 over the study area. Linear, quadratic, cubic and hidden trends were investigated in this work. It has to be mentioned that there were some areas with no significant trends, which in this thesis are shown as “no trend” areas. A significant trend is defined as a trend that is caused by a factor or factors rather than chance, tested

using a statistical significance test based on the T value. An algorithm developed by Jamali et al. (2014) was applied to detect the trends, and a MATLAB script was used to implement the algorithm. The general steps of the algorithm are shown in Fig.11.

The algorithm starts with fitting a cubic polynomial function on the dataset of phenology parameters. Three conditions are required to assign a trend as a cubic class. First of all, the cubic coefficient must be statistically significant, which means that the first coefficient must pass a t-test at confidence interval (in this work: 95%). The second condition is that a cubic trend must have both a local maximum and a local minimum. If one of these conditions fails, the algorithm tests a quadratic trend; otherwise a first order polynomial is fitted. In a case when the first linear trends statistically passes a t-test at the 95% significance level , the trend is assigned as a cubic class, which means that the trend has two optimal points, and the general trend is significant. However, rejecting the linear trend results in a cubic hidden trend. It means that although two distinct optimums (fluctuations) have occurred, no significant net change has occurred.

In the case that the cubic trend is rejected, a quadratic trend is tested. It follows the same procedure as the cubic trend, with the difference that only one minimum OR one maximum is required. Similar to the cubic trend, a first order polynomial is fitted, and a quadratic trend class is assigned to the pixel if the coefficient of the linear trend passes t-test at 95% of confidence interval; otherwise, a quadratic hidden class is assigned to the pixel.

In case of rejecting both cubic and quadratic trends, a linear trend is tested on the annual seasonality parameters. The only condition required for fitting the linear trend class is to check if the coefficient passes the t-test. If this is true, then the pixel is assigned to the linear class, otherwise, no trend class is assigned to the pixel.

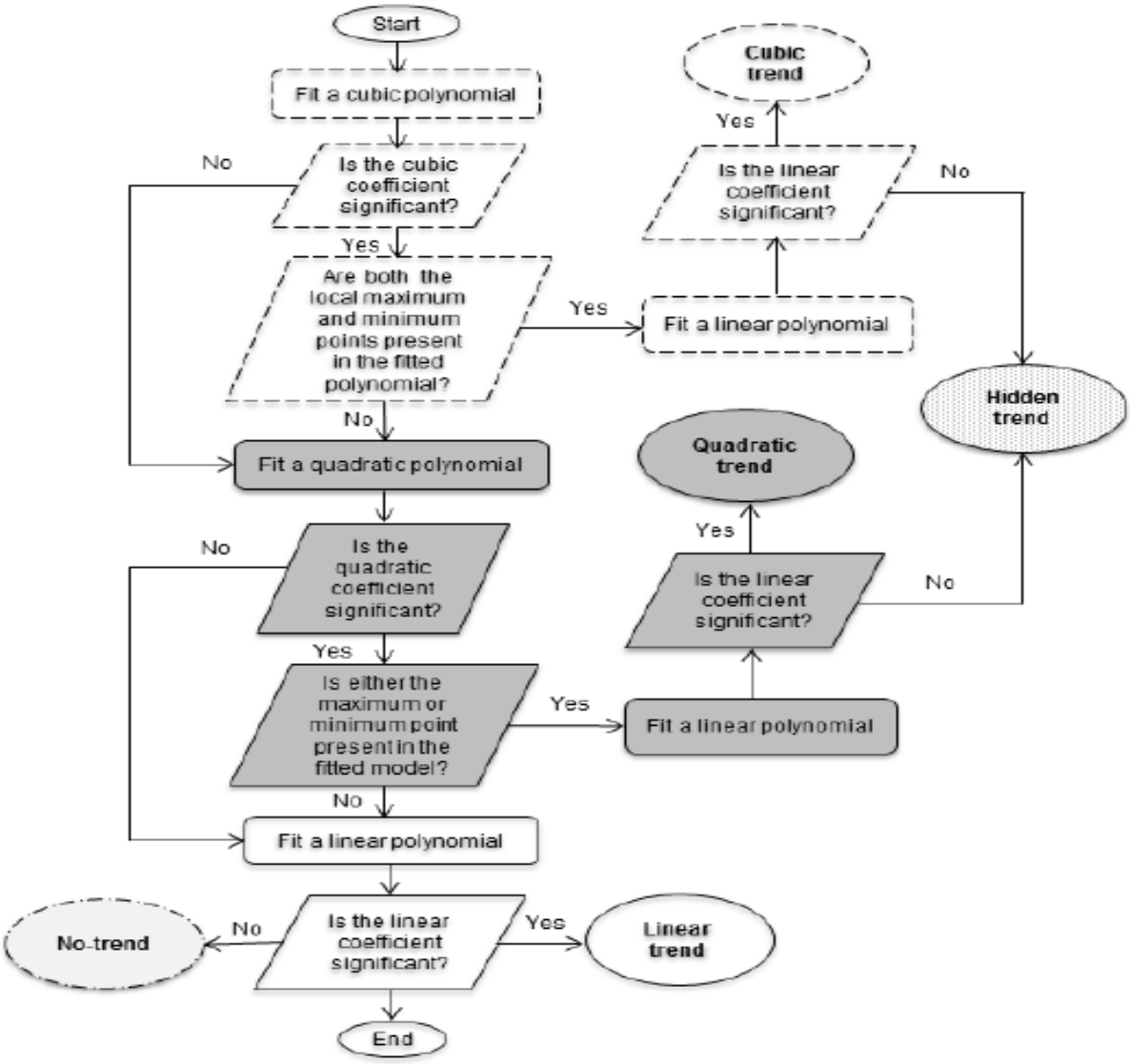

Fig.11.General steps to implement the linear, quadratic, cubic trend in addition to define the cubic hidden trend, quadratic hidden trend and no trend (Jamali et al., 2014).

The algorithm described above was implemented for five annual phenology parameters over the study area. Apart from the trend types, another parameter that was considered during the trend analysis was the magnitude of the higher degree polynomial trends.. The quadratic trend magnitude was defined as the differences between the maximum or minimum values of the quadratic trend and the linear trend value at the same time, as shown in Fig.12.

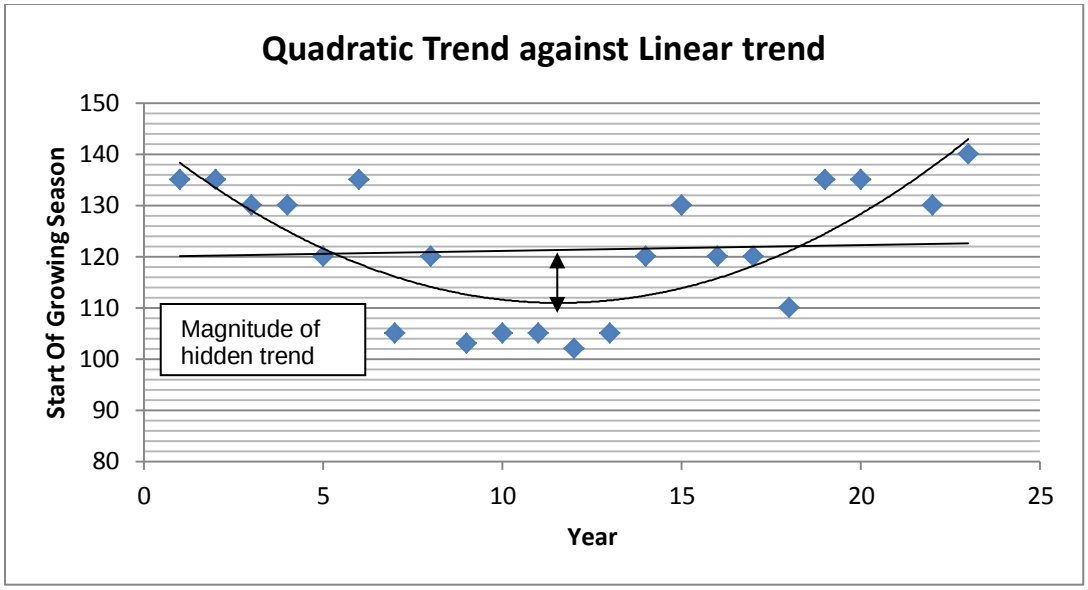

Fig. 12. Quadratic and linear trends of SOS against time. Double arrows sign shows the magnitude of a hidden trend.

Moreover, the year of optimum occurrences was derived for all quadratic hidden trends which refer to the year that had the lowest or highest value of a phenology parameter. Finally the results were imported in ARCGIS and masked to the study area.

MATLAB software version 7.12.0(R2011a) was used to calculate the trends of phenology parameters.

Note: regarding statistical analysis, accuracy of fits is affected by the number of observations; therefore those pixels which had more than five no-data values (of 23 total values) were excluded from the analysis.

2.2.2. Soil Moisture trends

The same algorithm was used to detect the trend types for all 12 months of soil moisture dataset. Polynomial and hidden trends for the period 1983-2005 were investigated over the study area.

2.3. Spatial comparison

Preparation of trend results of phenology parameters:

The binary format results from the phenology trend analysis were imported into ARCGIS. The spatial reference system of the resulted raster files were defined as Universal Transfer Mercator

(UTM) with geodetic ellipsoid of WGS84. The spatial resolutions of the results were 0.0727 º degree which is almost equal to 8 kilometers. The total region that was investigated as the study area covers around 11,000,000 Sq.km.

Preparation of mean phenology parameters:

The average of the derived phenological parameters (over 23 years) was calculated in Matlab. The results were imported to ARCGIS; afterward, were converted to raster format and defined as Universal Transfer Mercator (UTM).

2.2.3.1. Preparation of soil moisture trends

The binary format results from the soil moisture trend analysis were imported to ARCGIS and converted to raster formats. Since the spatial resolution of the soil moisture data was 0.5 degree, data was resampled to 0.0727 degree spatial resolution to be comparable with the phenology parameters. The soil moisture data was projected to UTM WGS84 reference coordinate system, and afterward was clipped to the study area.

2.2.3.2. Preparations of correlation maps

The phenology parameters from TIMESAT were tested for correlation against the resampled soil moisture data. For this purpose, the resampled soil moisture data of each month was correlated with the phenology parameters from 1983-2005,

From the trend maps, regions of occurrence of each trend kinds for SOS and EOS were identified. Also from the mean phenology parameters, the mean values of the parameters were defined. Afterwards, the relationship between the trend kinds and the soil moisture data for the corresponding time was investigated through the correlation coefficient. A p-value map was created to show the probability of no correlation, which means the probability of occurrence of a relationship by chance. Since SOS and EOS are directly affected by soil moisture, the correlation coefficient and the p-value analysis was only performed for SOS and EOS.

2.2.3.3. Data preparation for land cover, soil texture and rainfall

The land cover and soil texture maps were defined in UTM WGS 84 and clipped to the study area. These layers were overlaid on the map of phenology parameters in order to find the effects of driving forces behind the phenology changes.

2.3. Spatial comparison:

The results of the phenology trends were compared against the trend kinds of soil moisture to show their spatial relationship. Finally, through overlaying the data, the relationship between the results of the phenology parameter trends and the climate driving forces and soil texture were investigated.

Chapter 3

3. **Results and Discussion**

The results are discussed in three sections:

In the first part, the results of the mean phenology parameters values are presented and discussed. These results are valuable, because they display general spatial variation of the vegetation phenology parameters. In addition, these results are used to compare the phenology parameters against soil moisture and to find their correlation.

In the second part, the results of linear trends of phenology parameters are considered, and are compared with the previous results.

In the third part, the different polynomial trends, including cubic; quadratic; and hidden cubic and hidden quadratic trends are discussed, ordered by the phenology parameters. The results of SOS and EOS are compared against the polynomial trends of soil moisture time series for the same period as the phenology parameters. Through overlaying on the phenology results, rainfall and land covers as two factors that may contribute to the vegetation phenology trends, are considered and discussed. Finally, the map of soil types is spatially compared against the trends of phenology parameters.

*3.1. **Mean phenology parameter values***

3.1.1. Results

Fig. 13 shows the mean occurrences of phenology parameters from 1983 to 2005. Only one growing season per year was analyzed in this project; therefore, the analysis ignored possible variation in the secondary production of herbage.

SOS generally started from February in the south to August in the northern latitudes (around 15º N) as shown in Fig.13A. Except for local variations, the mean SOS followed rainfall and land cover patterns (compared with Figs. 3 and 4). The main occurrences of EOS, around 63.1% of the study area, occurred in November and December, particularly over the central parts (Fig.13B). The northeast regions, as well as some regions in the eastern countries (including east of Ethiopia, north of Kenya and Somalia) and those areas in the south dominated by evergreen forests (Fig. 3), were not distinctly separable due to low amplitude. The dominant land cover of northeast and eastern parts is sparse grassland and sand, with annual rainfall of less than 400 mm. The highest amplitude happened in the middle latitudes of the study area (Fig. 13C), where the areas are mainly covered by shrub lands, closed grassland and cropland. The general trend of LOS increased from north towards south, as shown in Fig. 13D. In addition, the general pattern of LOS generally followed the land cover and rainfall variations. SI had maximum values in those regions within maximum amplitude and longest length of growing season (Fig.13E).

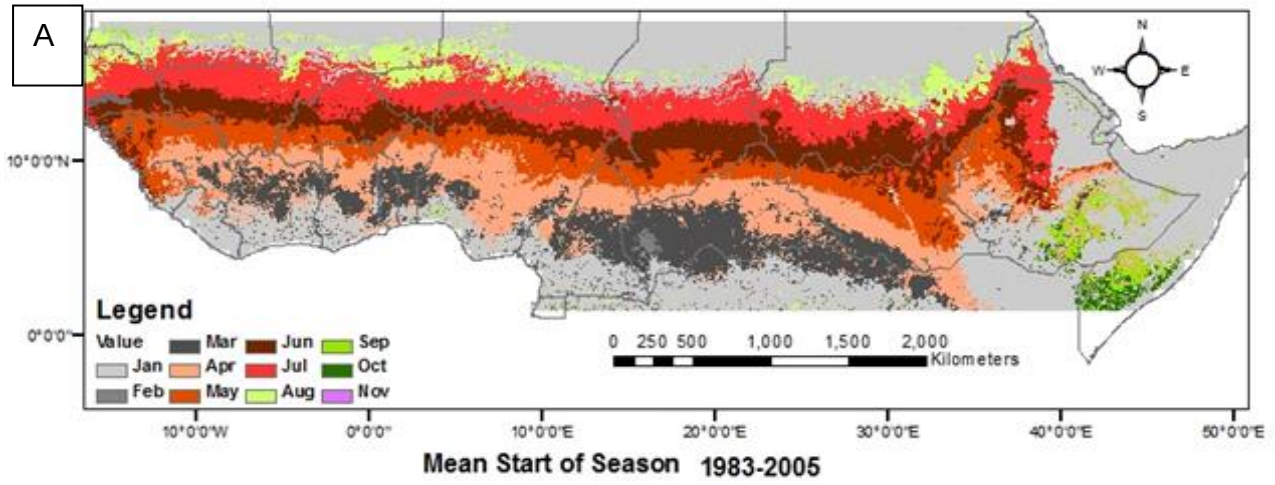

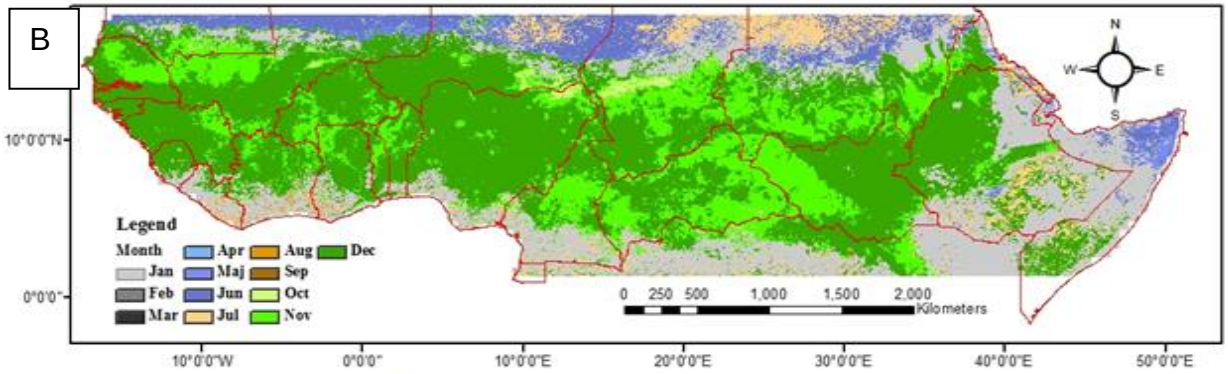

Mean End Of Season 1983-2005

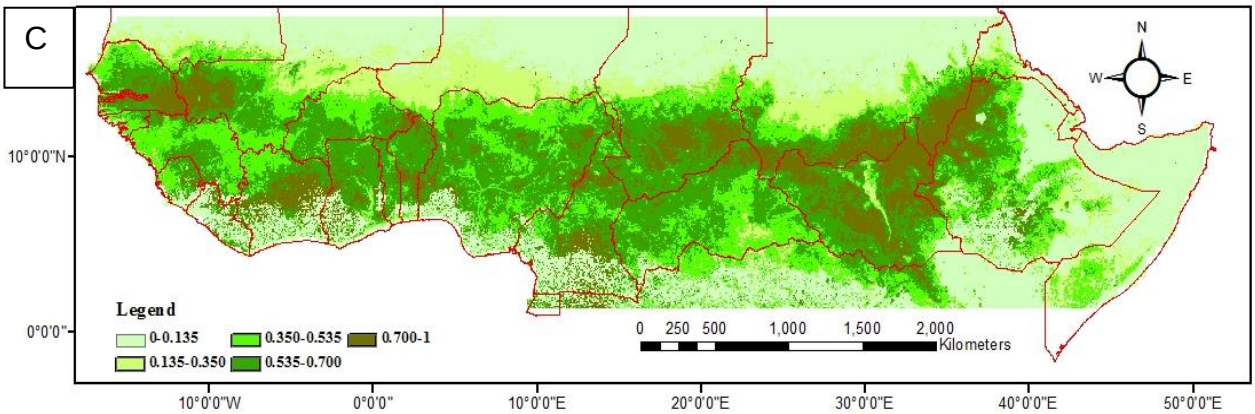

Mean Amplitude Of Season values From 1983-2005

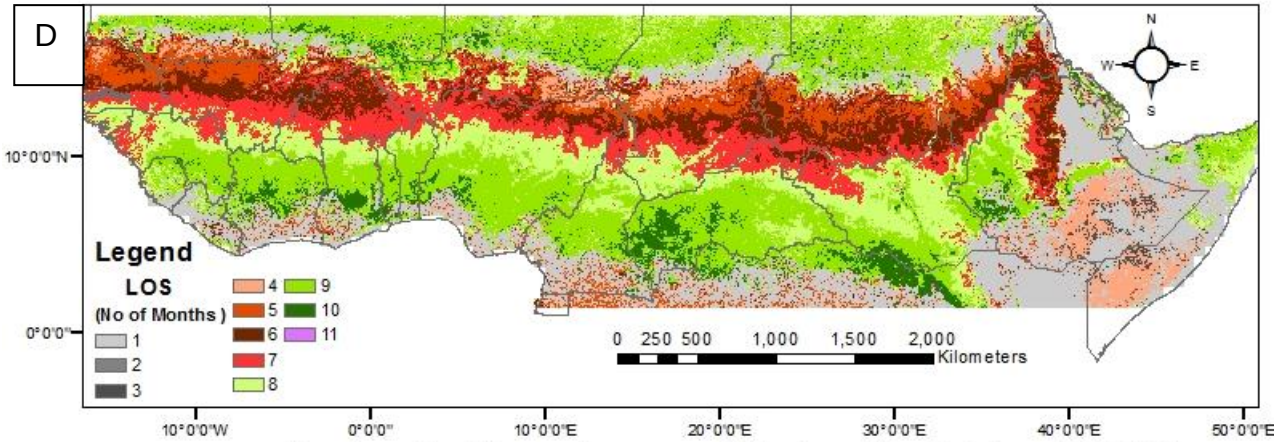

Mean Length of Season Occurrence (Number of Months) from 1983-2005

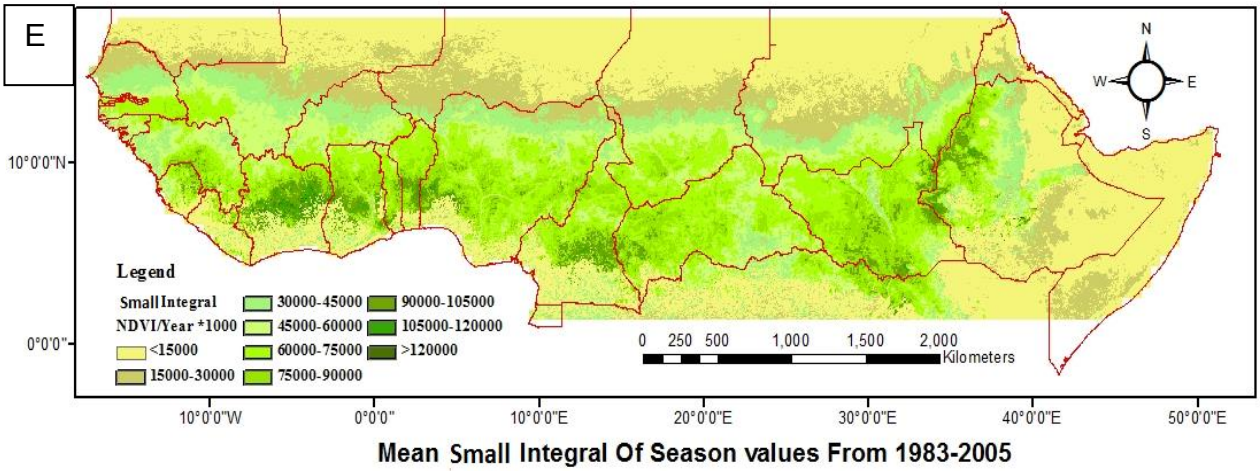

Fig.13.(A-E). Mean values of large integral of season from 1983- 2005. Start of Season (A), End of Season (B), Amplitude of season (C), Length of Season (D), and Small Integral of season (E) are shown.

3.1.2. Discussion

The results illustrate that seasonal phenology parameters derived from NDVI depicted the general increase of vegetation trends from north towards the south of the study area. However, some exceptions to these trends were found over the area such as the Ethiopian mountain regions, where vegetation decreased from high elevated regions towards cropland plains in both sides of the mountain chain.

The maximum length of growing seasons occurred over the Guinean zone and the mountain chain of western Ethiopia (Fig.13), from 9 to 10 months of greenness which were associated with annual rainfall and land cover patterns.

The results from the north-east areas as well as some regions in the eastern countries (including east of Ethiopia, north of Kenya and Somalia), and those areas in the south which are covered by evergreen forests (Fig.3) might not represent the real occurrence of phenology parameters. One reason for unrealistic values is climate factors and very low amplitude in the north-east and the eastern regions. For instance, weather in Ethiopia and Kenya is affected by ITCZ and circulation over the Indian Ocean and Arabic peninsula. Since the regions are located in dry climate with low annual rainfall of less than 400 mm, it has resulted in low NDVI values as well as a very short

growing season period. The dominant land covers of these areas (sparse grassland or sand) convey these characteristics. These circumstances make it hard to distinguish between NDVI and noise in the area. Moreover in such areas, NDVI values might have been affected by soil background reflection (Heumann et al., 2007) more than in the humid and sub-humid regions. In comparison with dry areas, distinguishing variation of phenology parameters over the evergreen forests areas was difficult, because of low fluctuation of NDVI during the growing seasons (Fig.13).

The highest amplitude occurred in the middle latitudes (Fig. 13D). This was anticipated, since land cover of the area has fast response to rainfall variation compared to other areas such as deserts and evergreen forest. Regarding vegetation production, local variation might be due to the land cover of the area, soil texture characterizations as well as variation in topography and human contribution.

3.2. Linear Trend of Phenology Parameters

3.2.1. Results

Figure 14 shows the spatial distribution of linear trends for five phenology parameters over the study area. Negative, positive and not significant classes were distinguished over the study area for the period of 1983 to 2005. Negative and positive trends of SOS and EOS refer to early and late start and end of growing seasons, respectively.

Positive linear trends of phenology parameters have occurred in different climate zones. The Guinean zone, including some parts of Central African Republic, Cameroon, Burkina Faso, Guinee, Mali and central Nigeria have had positive linear trends of EOS and LOS, while AMP and SI have mainly increased over the Sahelian zone. Central Nigeria and north of Central African Republic were two large clusters wherein EOS has been delayed as shown in Fig. 14B. LOS in Central African Republic as a main cluster in the Guinean zone has increased by up to 1.5 day per year (Fig.14C). The significant increase of AMP was found over the Sahelian zone, including central Chad, regions in the border of Burkina Faso and Mali, and some scattered areas in Mauritania (Fig.14D and Fig. 14E). These regions are dominated by cropland with relatively low

annual rainfall. Maximum increase of SI was mainly recorded over cropland areas of the Sudano-Sahelian zone.

Significant negative trends of SOS, EOS and LOS were mainly found in the Sahelian zone except a deciduous woodland cluster in Guinean zone of the east of Central African Republic (Fig.14) wherein SOS has decreased. The main clusters of these changes were located in the border of Sudan and Chad, Central Chad and an area near the border of Mali and Burkina Faso (Fig. 13). These areas which are mainly covered by grasslands with mean AMP of less than 0.35 NDVI units have experienced annual rainfall of less than 400 mm (Fig. 5). Substantial decrease of AMP (1.0% per year) was found over the Guinean zone in Cameroon, Cote d'lvorie, Liberia, Sierra Leone and Guiana with annual rainfall of 1000 to 2000 mm (Fig.14D). The areas are dominated by deciduous woodland and mosaic forests. SI has decreased over the same zone as the amplitude, but to a lower extent (Fig. 14E).

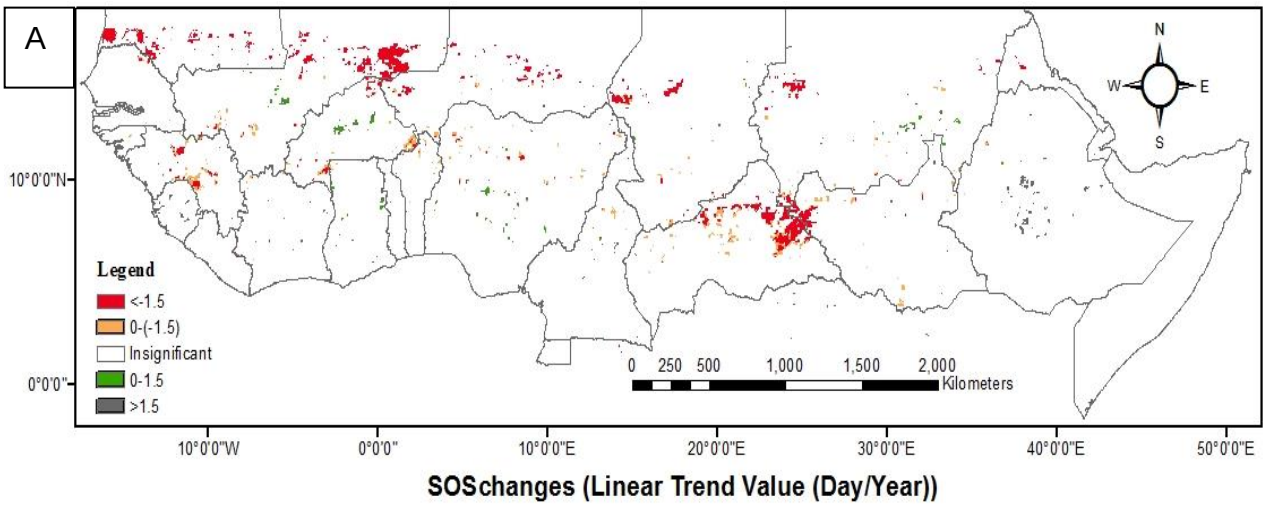

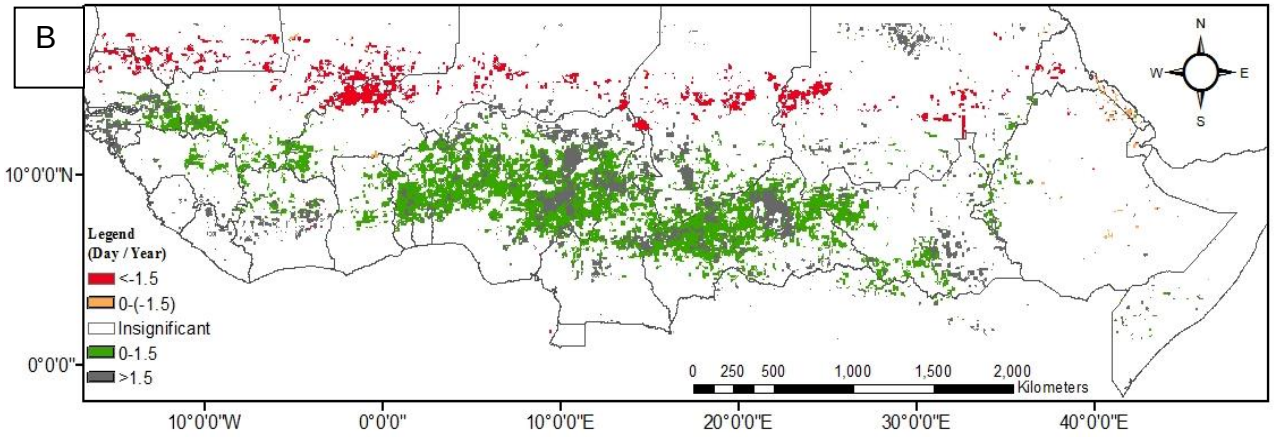

EOS changes(LinearTrends value(day/year)

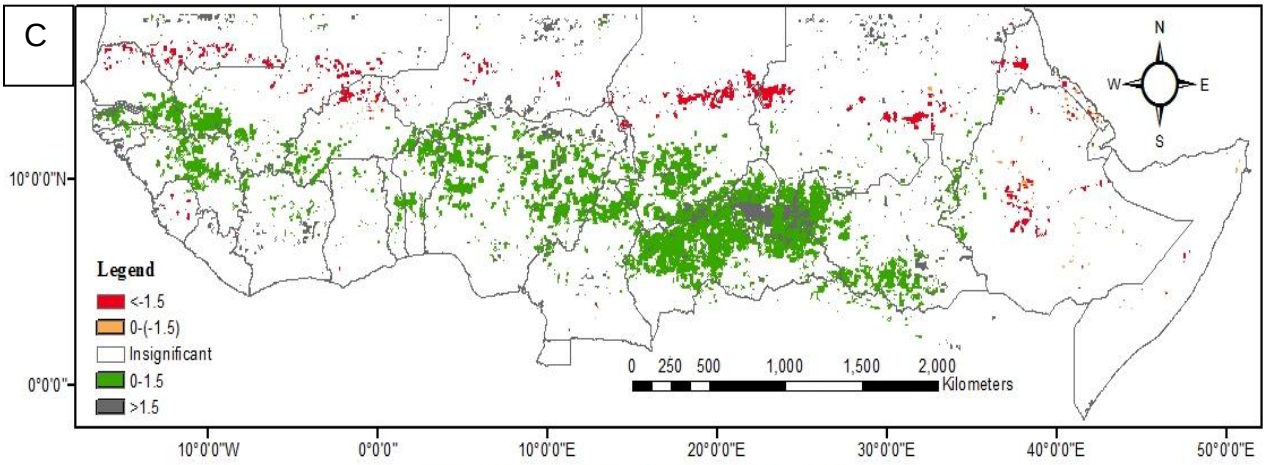

LOS changes (Linear Trend Value (Day/Year))

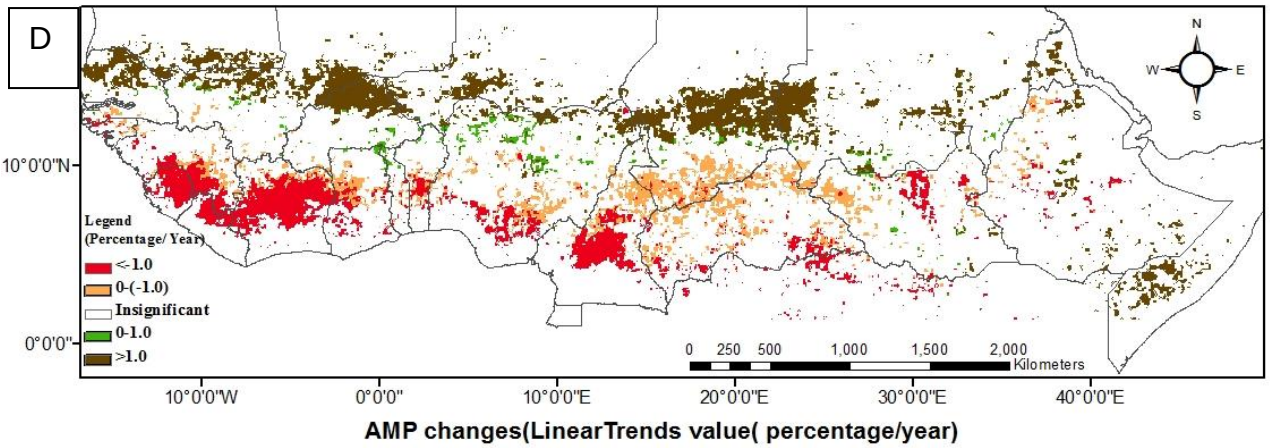

AMP changes(LinearTrends value(percentage/year)

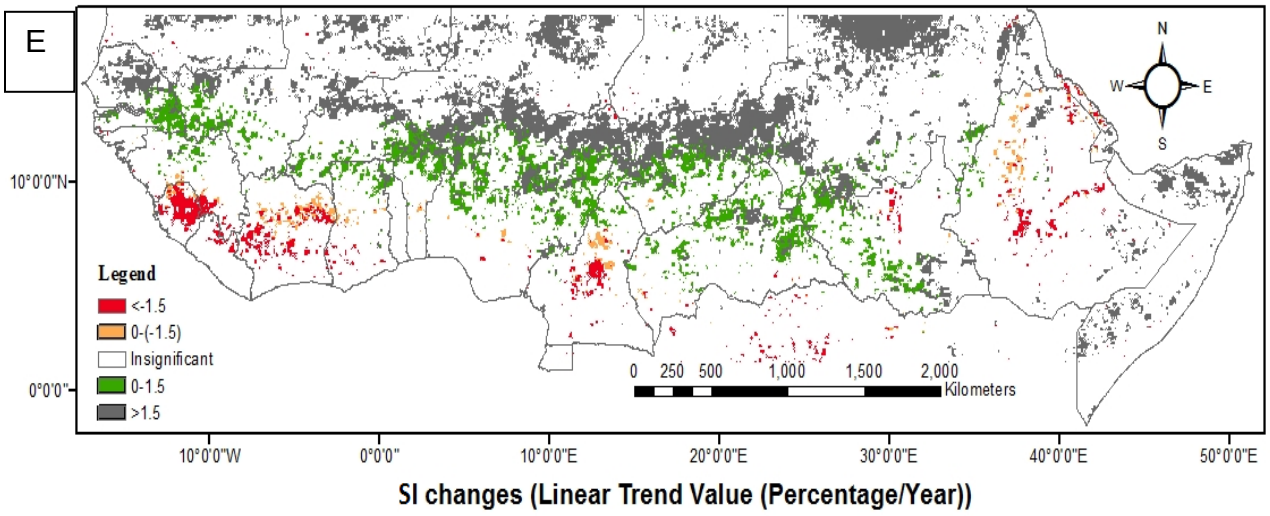

Fig.14. (A–F): significant trends of SOS (A), EOS (B), LOS (C), AMP (D), and SI (E).

3.2.2. Discussion

The magnitude of the negative linear trend of SOS in both clusters, one month advance over the 23 years, as shown in Fig. 14A, is remarkable. An earlier start of season in Mali has resulted from an increase of the mean annual rainfall over the area (Huber et al., 2011), while due to no significant changes of rainfall over the Central African Republic, the early start of growing season is not explained through this factor. These two clusters were not detected in Heumann et al. (2007). The reason for the inconsistency might be due to different temporal resolution of the datasets. In addition, it might be because of their classifying the area into several land cover- based zones . Since only one method of extraction the parameters could not cover the variations of different land covers in the study area, classifying the area based on land covers may result in higher accuracy.

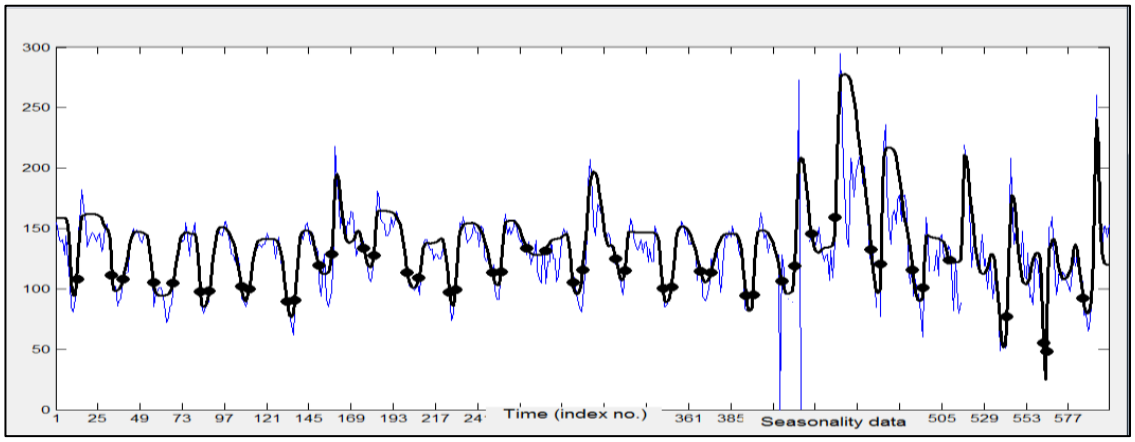

Fig.15. Time series of NDVI of a pixel in Eastern area in Mali using (raw data is in blue, TIMESAT fitted curve is in black). The NDVI unit is up- scaled 1000 times.

Since the maximum NDVI values in the Mali cluster were usually less than 0.2 units as shown in Fig. 15 (A sample point was selected in the border of Mali and Burkina Faso), the negative linear trend of EOS recorded in this area does probably not reflect any real change. The reason is high probability of noise in the NDVI data as well as the soil background effect. As shown in Fig. 13B, the magnitude of positive linear trend in EOS is substantial, particularly in the Central African Republic and central Niger. Moreover the results of positive linear trends of EOS were relatively well matched with the Heumann et al. (2007) results.

LOS has changed remarkably mainly over the Central African Republic, which is corresponds fairly well with reults of Heumann et al. (2007) and Jamali et al. (2014). Inconsistencies compared to the mentioned studies exist due to different temporal resolutions (10 days compared to 15 days in this work) and different procedures of extracting the parameters (classifying the area and applying calibration in Heumann et al. (2007) work).

Huber et al. (2011) found that the general trends of NDVI showed a significant increase in the Sahelian, Sudano-Sahelian and Sudanian zones. Variation in amplitude might be due to extending the season which led to increased differences between maximum NDVI and base line (Fig. 2) and/or changes in maximum NDVI. The increase of AMP in the Sahelian zone was due to a large increase in the maximum NDVI. However, significant decrease of AMP over the south east of the study area as well as central Cameroon was not anticipated, since no change of NDVI had been recorded (Huber et al., 2011); also no changes of SOS, EOS and LOS were recorded in those areas, as shown in Figs. 16 (A-C). However, the results were fairly consistent with the previous studies (Hermann et al., 2005, Heumann et al., 2007 and Jamali et al., 2014).

The map of SI linear trends was fairly consistent with Heumann et al. (2007) and Jamali et al. (2014). As SI is directly dependent on the amplitude and length of the growing season, the positive trend of SI seems reasonable due to remarkable increase of amplitude over the same area. Moreover, rainfall and soil moisture had increased from 1982 to 2007 in the regions which led to increase of SI (Huber et al., 2011).

However, there were substantial areas that did not experience significant linear changes of the parameters.

3.3. Polynomial Trends of Phenology Parameters

Figures 16(A-E) show computed polynomial trends of phenology parameters over the study area from 1983 to 2005. The changes of phenology parameters were mainly modeled with linear trends; however, there were a substantial percentage of phenology changes that was recorded as polynomial trends. However, "no trend" was found in large parts of the study area, as shown in Table.3.

Table 3.Percentages of different trends over the study area

	Positive linear	Negative linear	Quadratic	Cubic	Hidden Quadratic	Hidden Cubic	No trend
SOS	0.2	1.5	0.3	0.1	2.6	0.8	94.4
EOS	11.1	2.2	1.6	1.4	2.6	3.4	77.7
LOS	8.0	1.0	2.2	1.6	5.2	2.7	79.2
AMP	7.3	7.9	1.6	1.3	3.4	2.9	75.6
SI	13.8	1.6	2.3	1.4	4.6	3.2	73.1

Among the different polynomial trends, quadratic hidden trends had the largest proportions. The quadratic hidden trends could better explain the phenology changes than cubic and quadratic trends, since they were more frequent and occurred in clusters. As shown in Table.3, the cubic trend had the lowest proportion of phenology parameters.

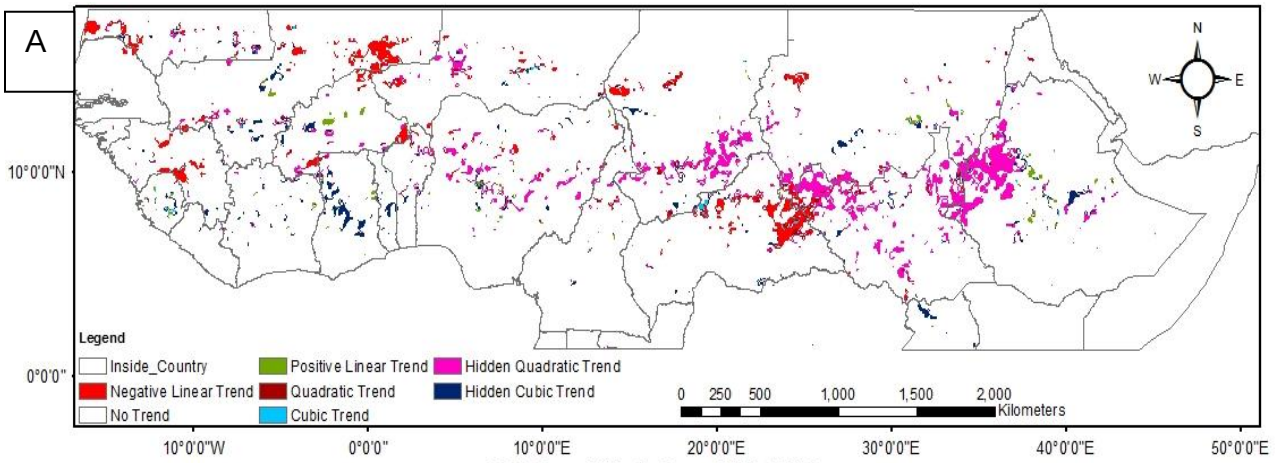

SOS Trend Kinds from 1983-2005

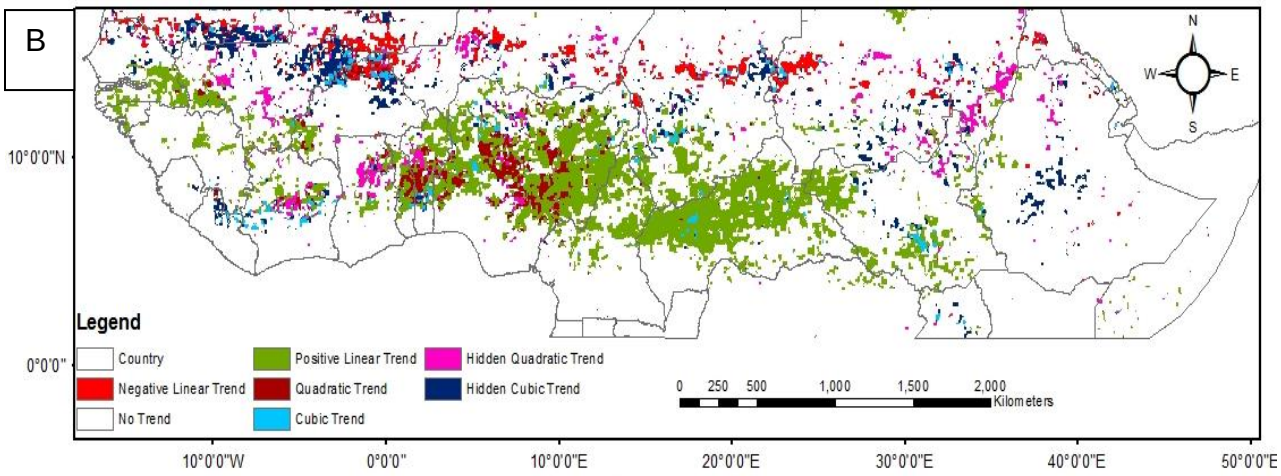

EOS Trend Kinds from 1983-2005

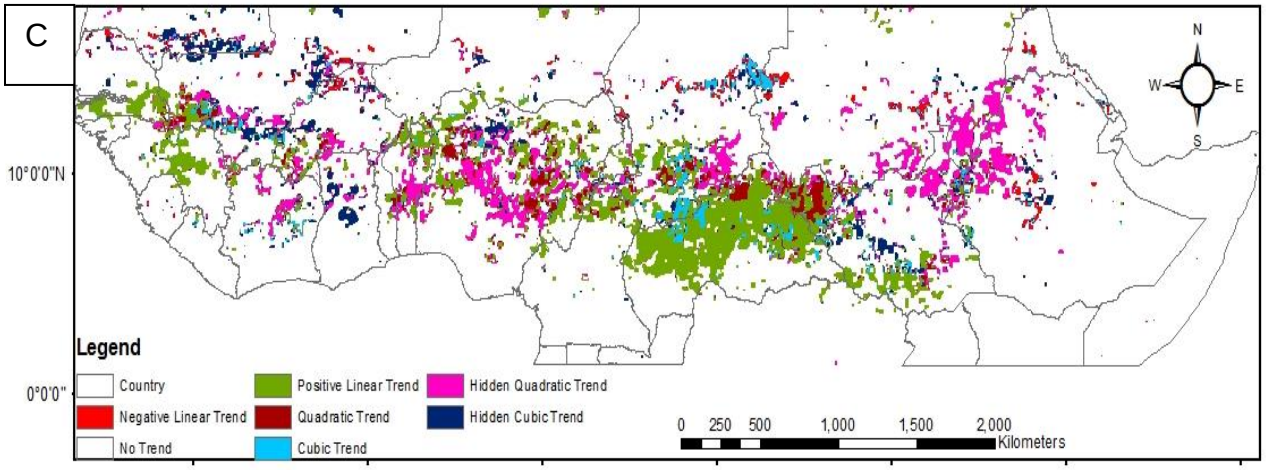

LOS Trend Kinds from 1983-2005

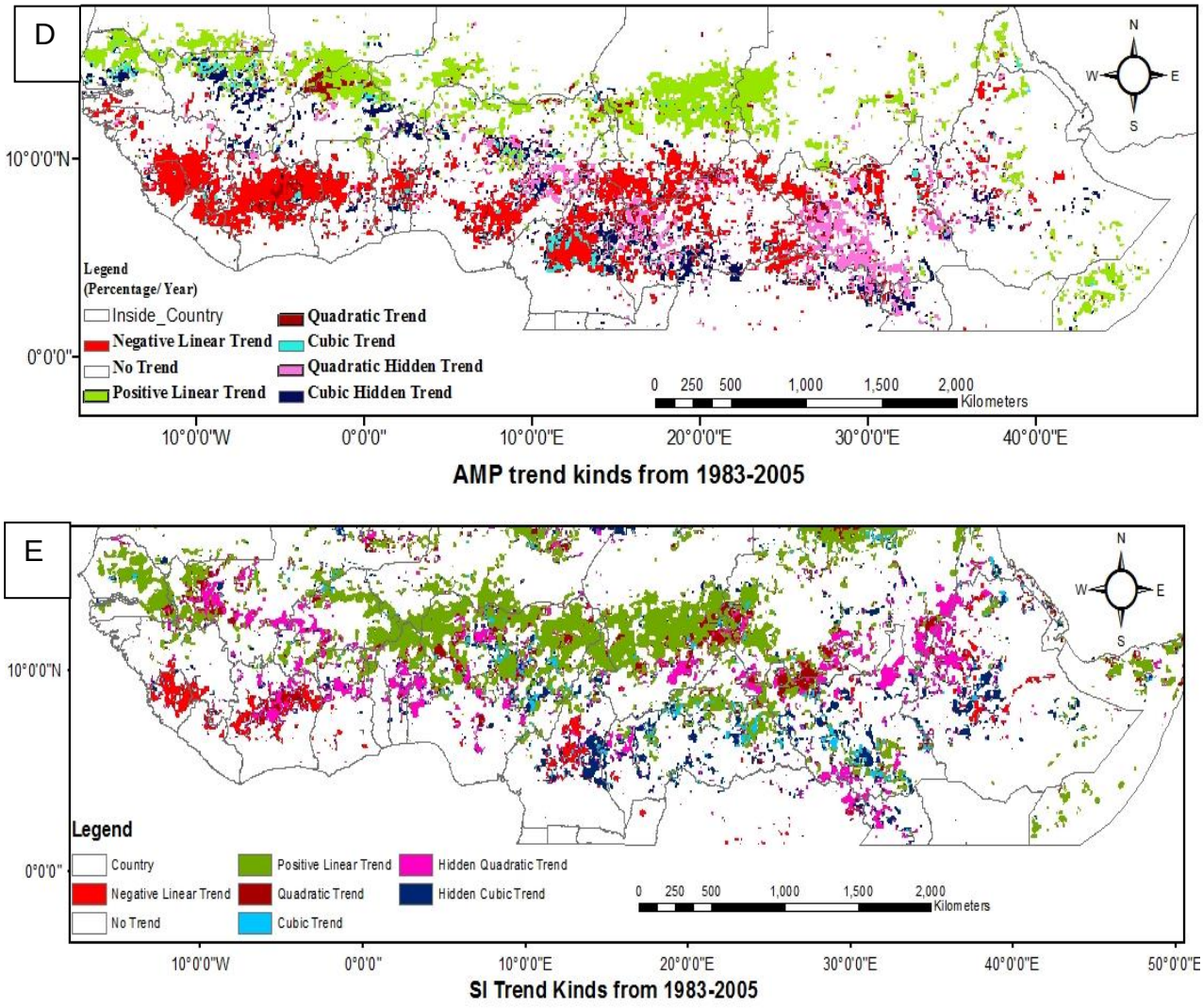

Fig.16. Polynomial trends of phenology parameters (negative and positive linear trends, quadratic, cubic, hidden quadratic, hidden cubic trends and no trend) over the study area from 1983 to 2005.

3.3.1. Polynomial trends of start of season

Figure 16A displays the polynomial trends map of SOS over the study area. Negative and quadratic hidden trends were recorded as the dominant occurring trends over the study area.

3.3.1.1. Results

Regarding the linear trend, two main areas in Mali and Central African Republic have experienced an advance of the growing season. The Mali area is covered with sparse grass with mean annual precipitation of less than 400 mm and Entisols soil type. No significant trends of AMP, LOS and SI were found for this region, while EOS has had a negative linear trend. Since the mean annual SOS

for this area begun in August, the correlation coefficient and p-value between SOS and soil moisture in August was calculated (Figs. 17 and 18).

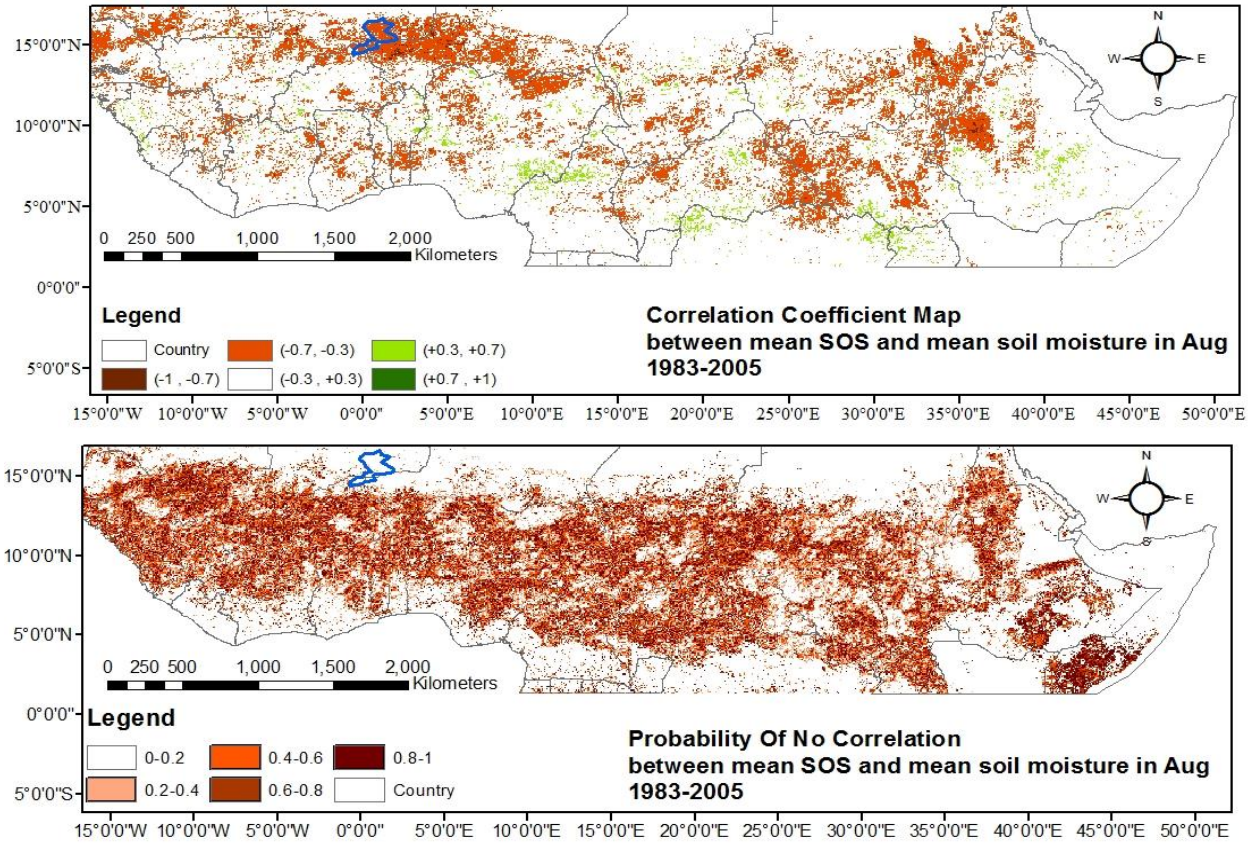

Fig. 17. (Top): Correlation coefficient between mean SOS and mean soil moisture in August.

Fig.18. (Bottom): P-value between mean SOS and mean soil moisture in August. The blue polygon shows the area with linear negative trend of SOS.

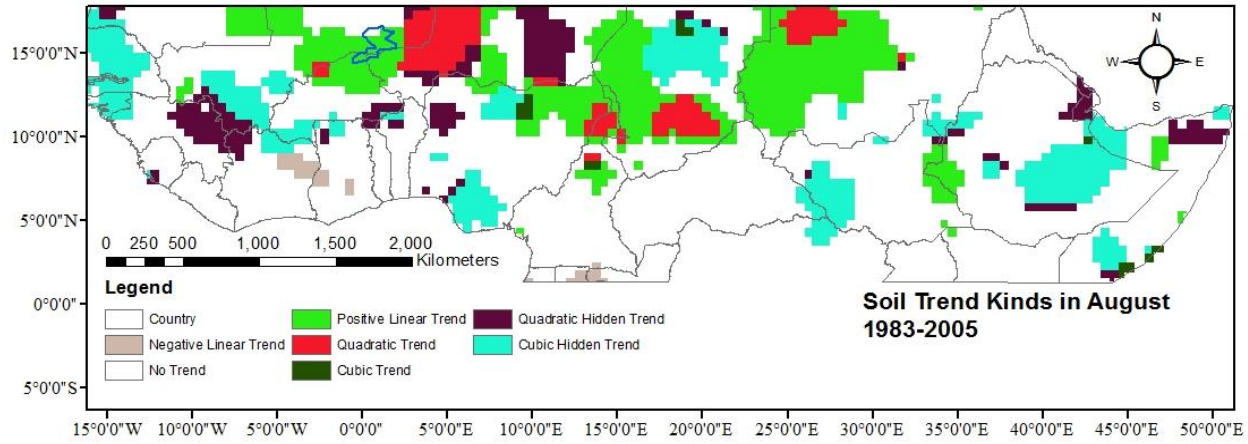

Fig.19. Soil moisture trend kinds of August from the studied period, 1983-2005. The blue polygon shows the area with linear negative SOS.

Moderate correlation (Fig. 17), between -0.7 and -0.3, with high probability of correlation (Fig.18) was found in the area. Also the positive trend of soil moisture in Mali relatively well coincided with the negative linear trend of SOS as shown in Fig. 18.

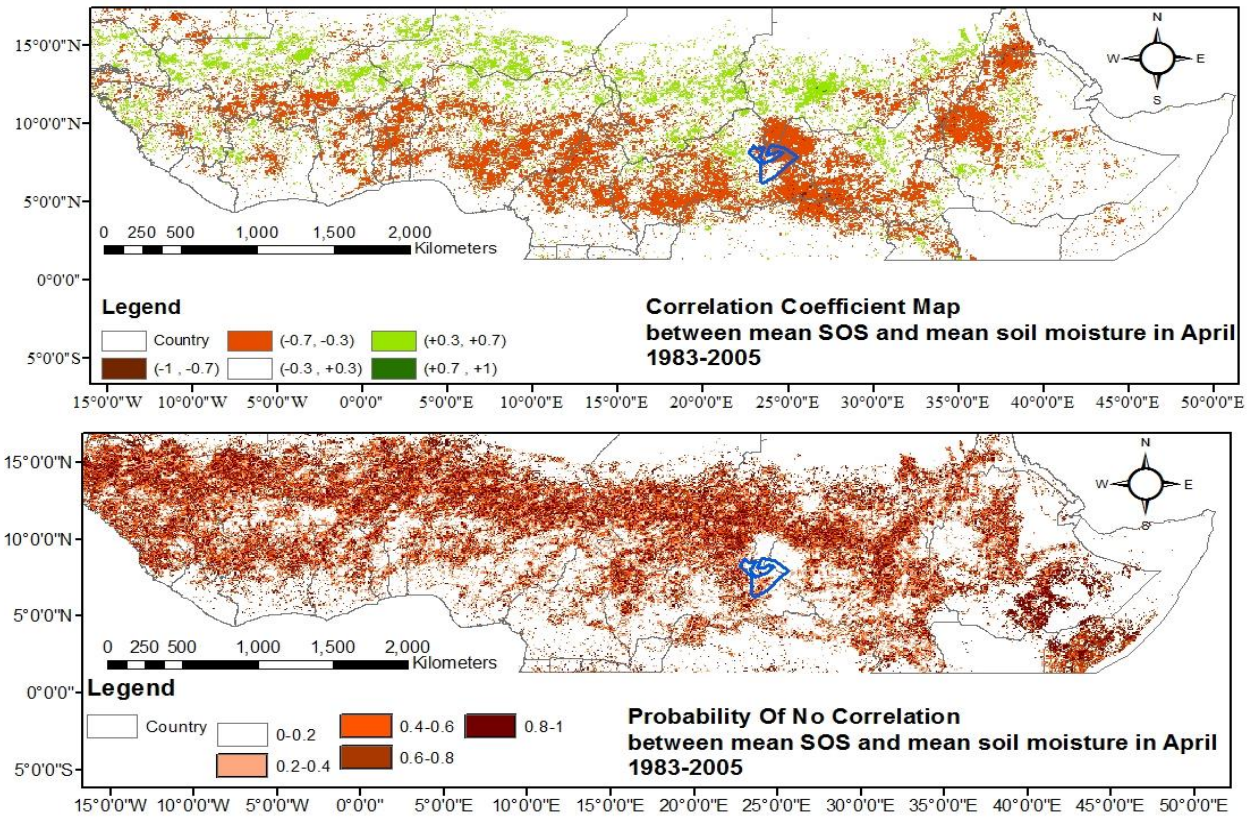

Fig.20. Correlation coefficient between mean SOS and mean soil moisture in April. Blue polygon shows the area with linear negative trend of SOS.

The other area that experienced a negative linear trend was located in deciduous woodland in Central African Republic, with mean annual rainfall of between 1000 to 2000 mm, and Oxisol soil type. The mean SOS of the area occurred in April. No significant correlation between soil moisture and SOS in April was found over the dominant part of this cluster, as shown in Fig. 20.

Infrequent and sparse quadratic and cubic SOS trends were found over the study area. However, only three areas of quadratic hidden trend were found, forming notable clustered regions, including the west of Ethiopia, north-west of South Sudan and the southern part of Chad, as shown in Fig.16A (light violet color).

The quadratic hidden trend of SOS was found mostly in deciduous shrub lands with sparse tree cover, mainly located in mountain areas of Ethiopia with soils of Alfisols and Inceptisols types. This area has had large annual precipitation, from 1000 to 2000 mm. In high mountain areas rainfall can reach 3000 mm. The second site has the same land cover, while its annual rainfall is between 600 and 1000 mm, and has soils of the Entisols class. Since the average time for start of growing the season in these two locations started in May, the correlation coefficient between mean SOS and mean soil moisture in May was investigated over the same period from 1983 to 2005.

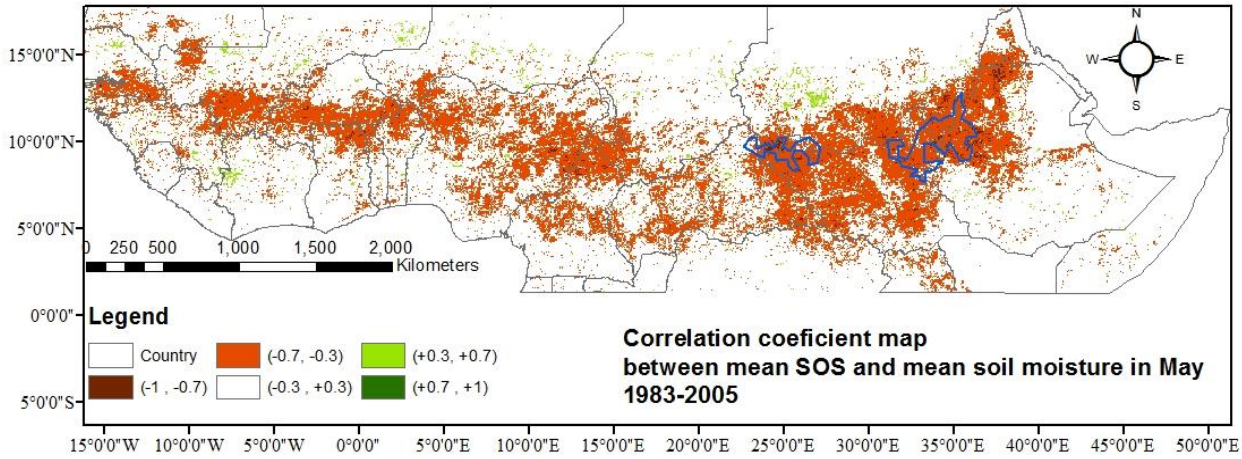

Fig.21. Correlation coefficient between mean SOS and mean soil moisture in August. The blue polygons show the area with quadratic hidden trend of SOS.

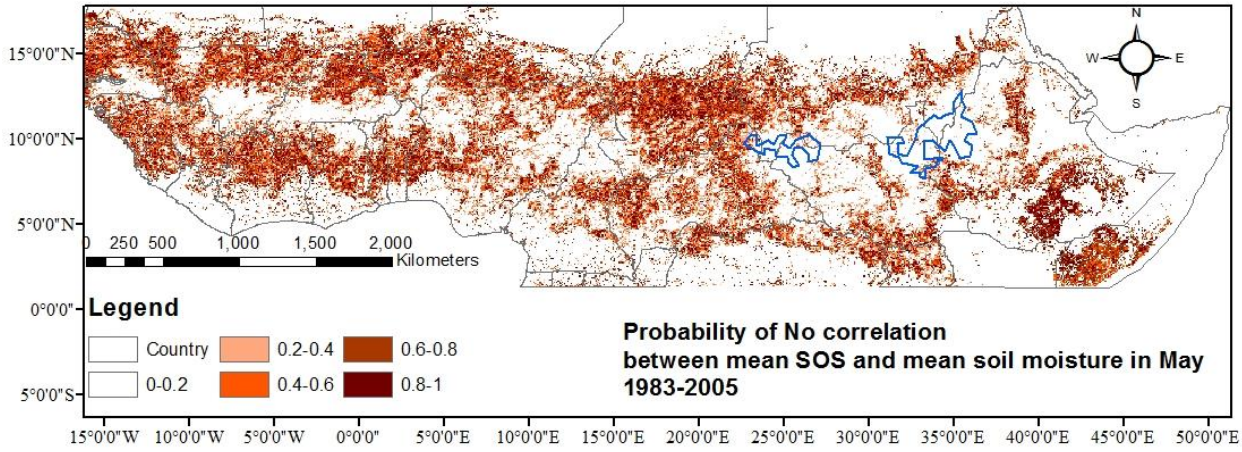

Fig.22. P-values between mean SOS and mean soil moisture in May. The blue polygons show the area with quadratic hidden trend of SOS.

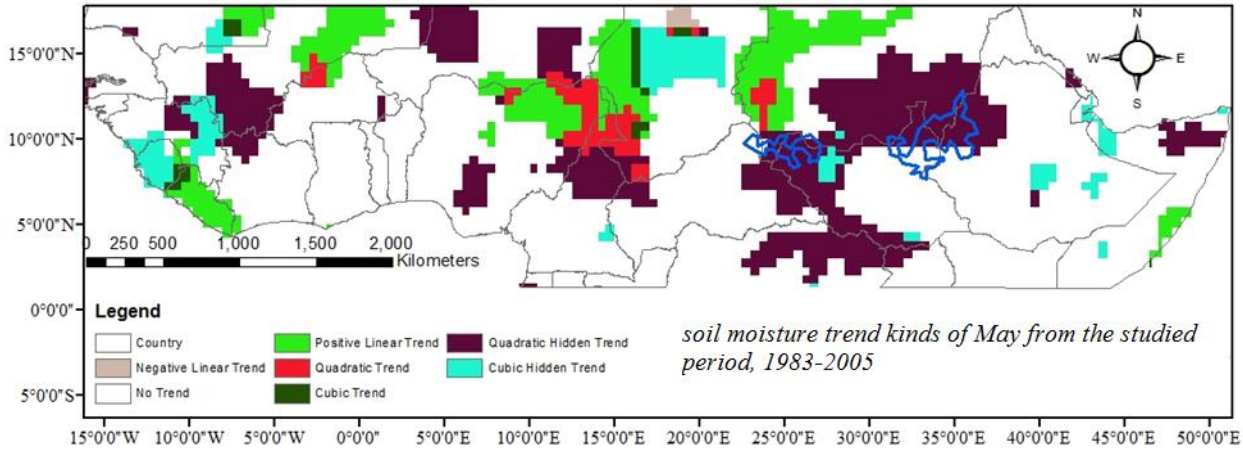

Fig.23. Soil moisture trend kinds of May from the studied period, 1983-2005. The blue polygons show the area with quadratic hidden trend of SOS.

A moderate correlation (-0.7- -0.3) between the variables was detected (Fig. 21), which was verified by p-value evaluation (Fig. 22). Moreover, soil moisture trend in May from 1983 to 2003 was similar to that of SOS (Fig. 23).

Another SOS quadratic hidden trend area was found in the south-east of Chad (Fig 16. A). The mean SOS in this area occurred in June, with annual precipitation of 600 mm up to 1000 mm, where it consists of open deciduous shrub lands, with Vertisols soil texture. In this area, only weak

significant correlation was found. Moreover, the trend of soil moisture was not the same as that of the SOS trend during the studied period.

Figure (24) displays the magnitude of quadratic hidden trend values of SOS. All three major clusters have experienced a negative quadratic trend with magnitude of 15 up to 30 days, which means that the growing season has tended to start earlier toward the minimum (earliest) SOS; after that, SOS has gradually increased (delayed) again (Fig. 12).

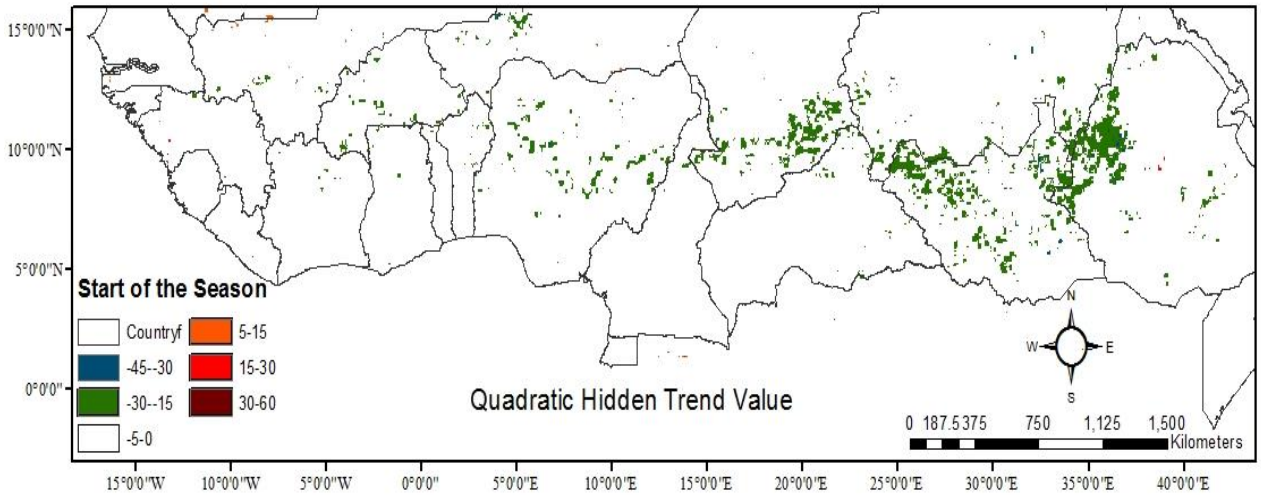

Fig.24. Quadratic hidden trend values of SOS over the study area from 1983-2005.

The optimal occurrence of a quadratic hidden trend was defined (in this work) as a year or a period during which the area has experienced the earliest (in this case) or the latest SOS. The optimal times of quadratic hidden trend of SOS, were classified into three main periods as shown in Fig.25. The results illustrates that the period 1993-1996 has had the earliest SOS for the studied area.

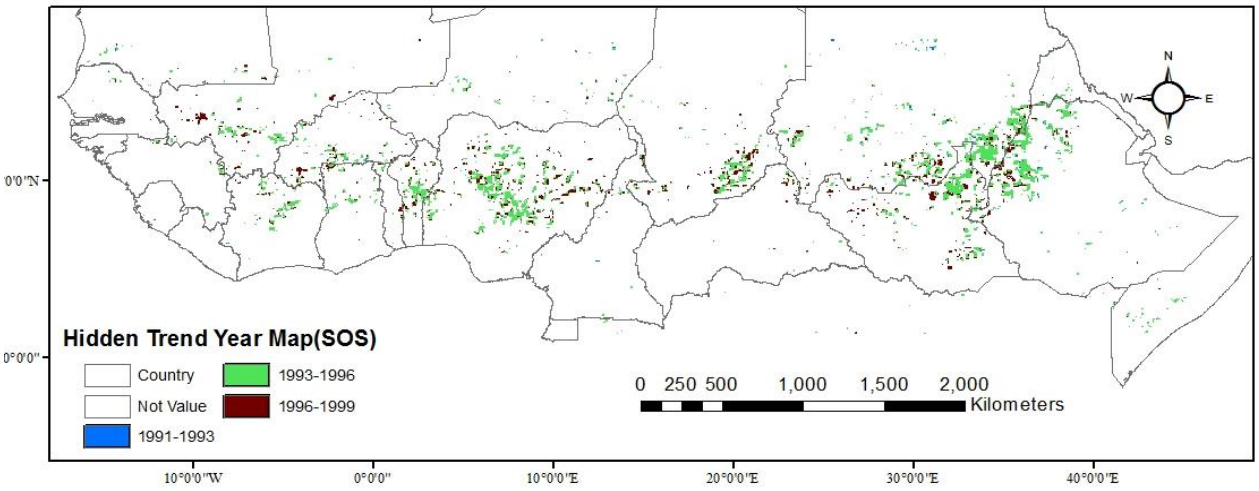

Fig.25. Occurrence of quadratic hidden trend in terms of maximum or minimum SOS.

3.3.1.2. Discussion

A negative correlation coefficient between SOS and soil moisture means that increasing the soil moisture corresponds to an earlier growing season, while a positive value reflects a later growing season. Significant correlation between SOS and mean annual soil moisture happened in August for the Mali cluster, displaying linear negative of SOS (Fig.17). The moderate correlation coefficient and p-value (less than 0.2) verified the high significance of correlation in August (Fig.17). Soil texture of the area is Entisols, which has been recognized as a soil type with largest contribution to vegetation changes over the study area (Ahmad, 2012). Occurring early SOS in in sandy soil areas of Mali was confirmed also by Kumar et al. (2002). While no significant change of AMP, LOS and SI was found in this site, an advanced EOS means that the growing season has largely had a shift towards an earlier occurrence without extending the season. However, the negative linear trend of SOS in the second site may not be reliable, since the only parameter that has increased was LOS (Fig. 16.C), and no changes of NDVI, rainfall and soil moisture were recorded over the region (Huber et al., 2011). Moreover, as shown in Fig. 19, there was no significant correlation between soil moisture and SOS in this site.

Regarding the quadratic hidden trends, soil moisture and SOS trends coincided in the first and second sites (western Ethiopia and north- west of South Sudan, respectively) while no coincidence was found in the third site (south-east of Chad). The reason for inconsistency in the third site

(south of Chad) might be due to the soil texture characteristics of the region (Fig.4), since this site has different soil texture in the region. As Vertisols have the ability to transmit water very slowly, it may have led to an earlier SOS. Significant moderate correlation coefficients, in addition to have the same soil moisture trends in the area indicates that soil moisture variation could explain the variation of start of growing season. However, quadratic hidden trend of soil moisture occurs over a considerably larger area than the SOS quadratic hidden trend. The reason may be differences in spatial resolution of the two data sets, and different techniques of achieving the data, as well as low accuracy of the soil moisture data set, since only few distributed ground stations for modeling the soil moisture data exist.

The results of the quadratic trend regarding SOS and EOS were considered together, because there might be a shift in only one parameter or shifts occur in both parameters. In the first case, the shift conveys the changes of the length of growing season based on direction of the phenology parameter change, while in the second case it depends on how SOS and EOS have changed. If both parameters change in the same direction (positive or negative directions), the results convey a complete seasonal shift. Otherwise, it leads to changes in the length of the growing season. Since no changes in EOS were recorded at all three sites, it is concluded that these areas have experienced the longest LOS during 1993-1996.

3.3.2. Polynomial trends of End of season

3.3.2.1. Results

Positive and negative linear trends, quadratic trends and hidden cubic trends were major kinds of EOS trends that occurred over the study area, as shown in Fig. 16B.

Early occurrence of linear EOS trends was located in several clusters in the Sahelian zone. These clusters were dominantly found in Mauritania, border areas of Mali, Niger and Burkina Faso, Chad and Sudan. This trend was found mostly in grass lands with Entisols soil type and low annual rainfall between 200-400 mm. The moderate negative correlation between EOS and soil moisture in November was recorded in the areas, except in Chad wherein the correlation was found as positive (Fig. 26).

EOS was delayed predominantly in areas with relatively high annual rainfall, from 600 to 2000 mm (Figs 5 and 16 B). The positive linear trend of EOS occurred particularly in the Sudanian and Guinean zone, and extended southwards from deciduous shrub lands and cropland to the mosaic forest lands, with dominant presence of Alfisols and Oxsisols soil types. Since the mean occurrence of EOS was in November and December, the correlation between soil moisture and EOS in November was considered. The correlation between EOS and soil moisture had decreased from north to the south of areas wherein EOS had been delayed. While moderate significant correlation between soil moisture and EOS was found over the northern parts of Central African Republic, Cameroon, Niger and south east of Mali, no correlation were recorded over the central and south regions of these countries (Fig. 26).

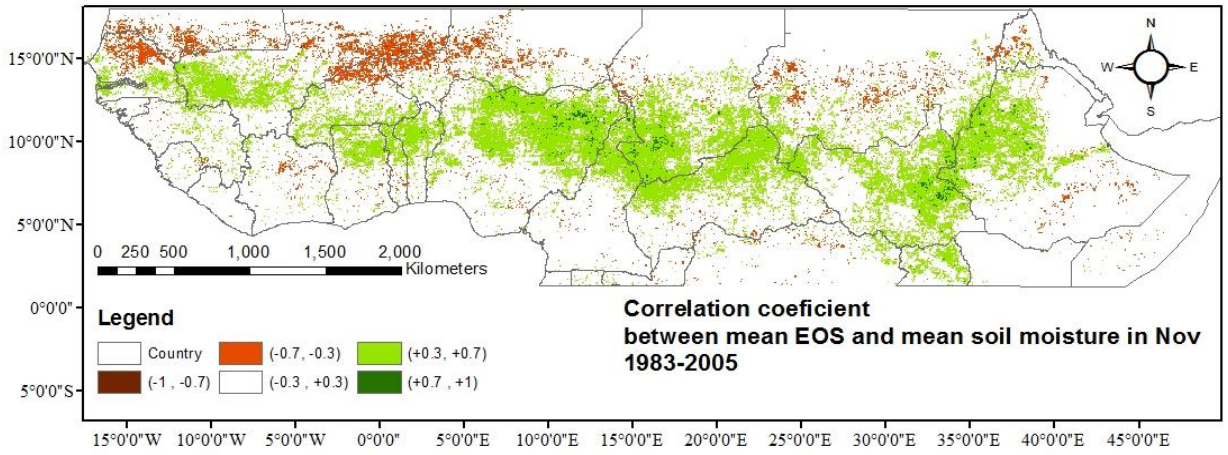

Fig. 26. Correlation coefficient between mean EOS and mean soil moisture in November.

Quadratic trends mainly occurred in cropland and deciduous woodland, of central Nigeria,and in Benin and Togo, respectively These two clusters have Oxisols soil type, and are located in the humid area with annual rainfall between 1000 and 2000 mm. Since the mean time of EOS in central Nigeria, Benin and Togo was in December, the results were compared with the soil moisture data in December. The results showed moderate significant correlation between the soil moisture and EOS in these areas. Moreover, the soil moisture followed the same trend as EOS.

The cubic hidden trend of EOS was frequently found in the same areas as the negative linear trend. The results indicated that Sahelian zone has experienced remarkable fluctuations of EOS regarding cubic and cubic hidden trends.

3.3.2.2. Discussion

Regarding areas with negative linear trend of EOS: since SOS had been delayed, while no changes of LOS and SI were found, the results are interpreted as a shift of the whole growing season. Moreover, since rainfall and soil moisture had increased by around 100 to 200 mm (Huber et al., 2011), and AMP had increased (Fig.16); the early EOS in these regions might occur because of a shift towards earlier dates in the rainfall distribution. Considering the increase of rainfall, the negative correlation between EOS and soil moisture might be due to low accuracy of the soil moisture data in the region.

The maps of positive linear trends matched those of previous studies (Heumann et al., 2007 and Huber et al., 2011), particularly in the north of Central African Republic where a significant positive correlation between soil moisture and EOS had been recorded. However, weak correlations in the southern parts of these countries might be because of low accuracy of the soil moisture dataset compared to EOS. Nevertheless, the results of soil moisture trend kinds in December (Mean occurrence of EOS), illustrated that EOS has followed changes in soil moisture relatively well.

For areas that have quadratic and hidden quadratic trends of EOS, due to the similar geographic and climate characteristics with the surroundings, and also the areas had the same soil moisture trends as EOS trends in addition to find the positive correlation between soil moisture and EOS, it is hard to highlight the land cover or soil types as drivers behind occurring these trends. The occurrences might be interpreted based on variations in rainfall regimes of the regions. Although considerable areas could be modeled with hidden cubic trends, there was no significant correlation between the soil moisture and EOS in those areas. However, sporadic occurrence of the hidden cubic trend might happen by chance (defined 5% as confidence interval in this thesis).

3.3.3. Polynomial trends of length of Season

3.3.3.1. Results

Fig. 16C illustrates the trend class map of LOS over the studied time period. Positive linear trends (7.9 % of the whole study area), quadratic hidden trends (5.1 %) and cubic hidden trends (2.5 %) were three major recorded trends in the middle latitude, mainly around north latitude of 10º.
There were also clusters of other trend types including negative linear trend (0.9 % of the study area), quadratic trend (2%) and cubic trend (1.42%), while about 80 % of the study area had not experienced significant changes.

Positive linear trends were found mostly in some parts of Central African Republic, Nigeria, and western countries of the study area (Fig .16C).

Table 4. Five main land covers wherein positive linear trends have occurred, considering their soil textures. Only 5 first major land cove types and three first main soil types which had a high percentage are shown in the table.

5 Main Land Cover classes with Positive Linear Trend of LOS
(only first three major soil texture types were considered)

	Land Cover	Mean Annual Precipitation (mm)	Soil Texture	Percentage	Total Percentage of the trend including all soil texture
1	Deciduous woodland	1000-2000	Oxisols	13.6	31.26
			Entisols	7.3	
			Ultisols	5.5	
2	Deciduous shrub land with sparse trees	1000-2000	Entisols	8	20.44
			Alfisols	6.7	
			Ultisols	3.4	
3	Mosaic Forest / Savanna	1000-2000	Oxisols	10.7	14.12
			Entisols	2.5	
			Ultisols	0.7	
4	Cropland with open woody vegetation	600-1000	Alfisols	5.2	12.31
			Entisols	4.1	
			Vertisols	1.7	

			Alfisols	2.6	
5	Cropland (>50%)	600-1000	Entisols	2.1	6.4
			Vertisols	0.8	

Deciduous woodland with mean annual precipitation more than 600 mm, mainly located in Central African Republic, Guiana and some parts of Nigeria, was the major land cover that was found to have positive linear trends (Table.4). Among different soil types which were covered by deciduous woodland, the oxisols had the maximum contribution (13.6 % of the entire positive linear trend). Other subclasses of land covers with major contribution to positive linear trend were deciduous shrub land with sparse trees and the savanna region, with annual precipitation of 1000-2000 mm.

To sum up, Oxisols with 24.3 % and Entisols with 24% were two main soil classes wherein the positive linear trend of LOS had occurred.

Quadratic hidden trends were recorded in 5 main areas with different characteristics. The results were overlaid on land cover and soil texture maps of the area in order to display the distribution of the trend over the land covers and soil texture, as shown in Figs 27 and 28. Regarding LOS, quadratic hidden trends mostly happened in deciduous shrub lands with sparse trees. As shown in Fig. 28, different soil types were found to have quadratic hidden trends of LOS, including Incepticols, Vertisols and Alfisols, while no distinct variations of soil texture were found inside these sites.

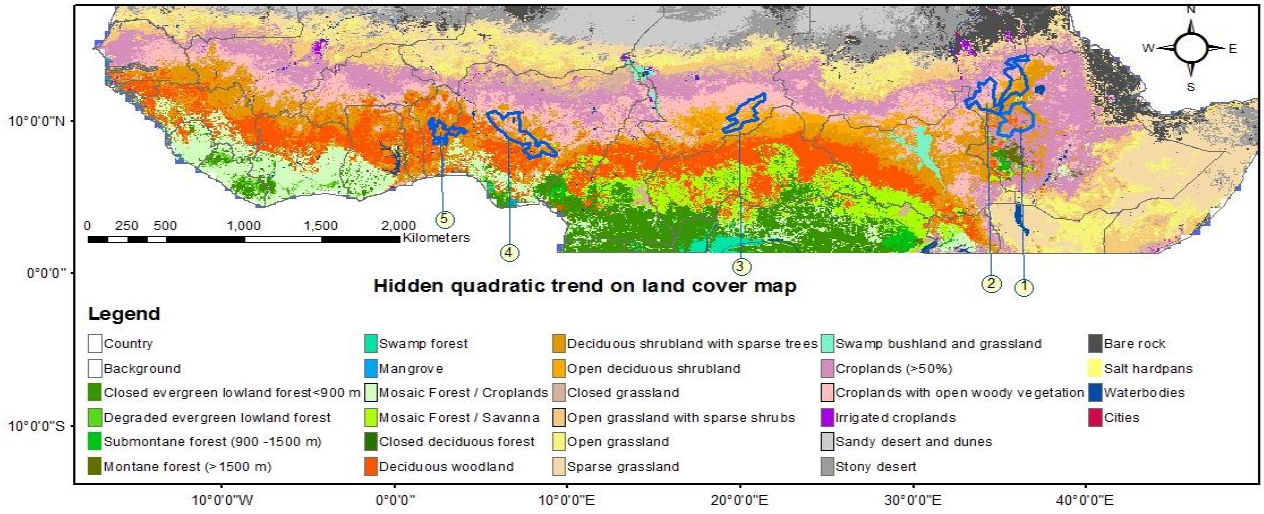

Fig.27. Distribution of 5 clusters of LOS quadratic hidden trend over the land covers.

Among these areas, site number 2 had the shortest LOS (5 to 6 months), while sites number 1, 4 and 5 had experienced the longest LOS (about 9 months), as shown in Table.5. Site number 3 had also relatively short LOS compared to other areas.

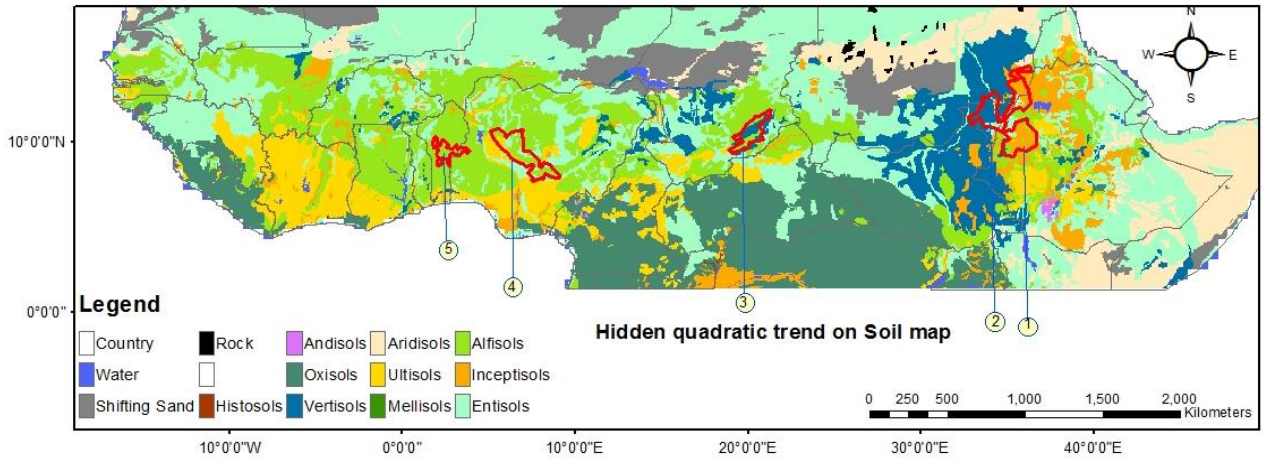

Fig.28. Distribution of 5 clusters of LOS quadratic hidden trend over the soil map.

Table 5. Summary information of the above 5 sites having experienced quadratic hidden trend of LOS.

Site	Mean annual precipitation (mm)	Dominant Land Cover	Main Soil Texture	Mean annual of LOS (number of months)
1	1000-2000 , some areas up to 3000 mm	Deciduous shrub land with sparse trees	Inceptisols	9
2	600-1000	Cropland with open woody vegetation	Vertisols	5-6
3	600-1000	Deciduous shrub land with sparse trees	Vertisols	7
4	1000-2000	Deciduous shrub land with sparse trees	Alfisols	9
5	1000-2000	Deciduous woodland & , Deciduous shrub land with sparse trees	Alfisols	9

Only site number 2 had experienced a strong increasing of LOS, between 15 to 30 days, and other sites had increased by less than 15 days. Maximum increase of LOS was found in the period of 1993 to 1996.

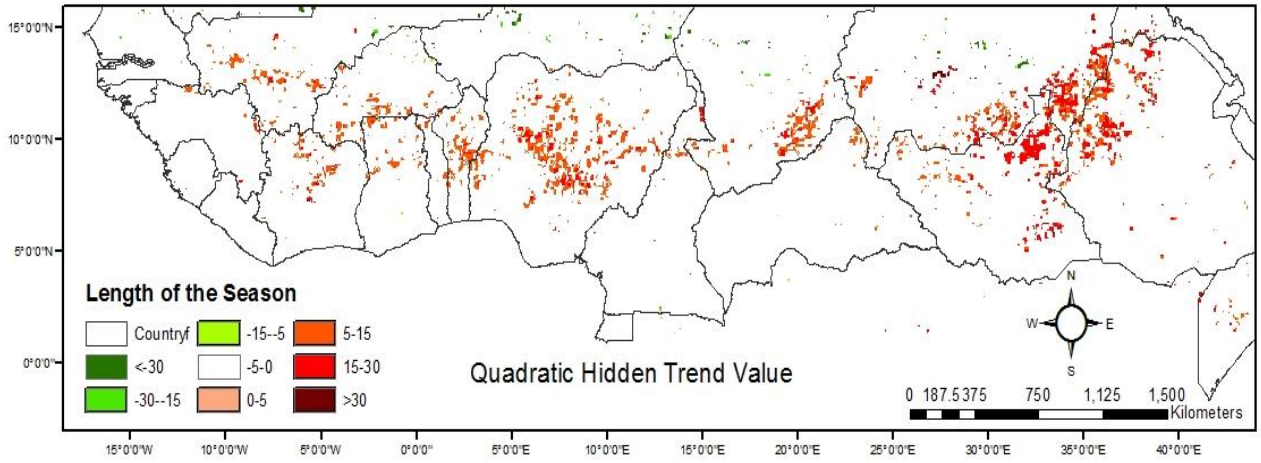

Fig.29. Quadratic hidden trend value related to LOS over the study area during the time period of 1983-2005.

Figure (30) illustrates the spatial distribution of cubic hidden trends in relation with land cover of the study area. Six major sites with occurrences of cubic hidden trends, covering approximately 2.5% of the study area, were scattered across different countries.

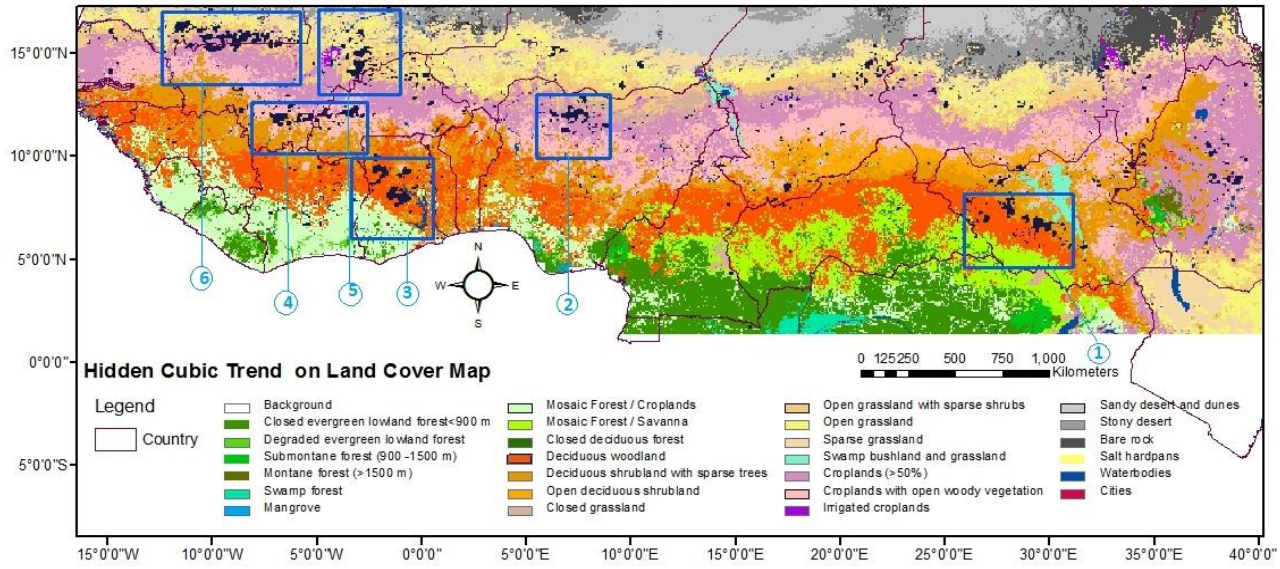

Fig. 30. Land cover map in relation with the occurrence of cubic hidden trend of studied time period.

However most of these sites were located in the western countries of study area between 10ºE and 15ºW, but in different climate zones.

Table 6. Information about 6 mentioned sites regarding land cover, soils and annual precipitation, which have experienced the cubic hidden trend of LOS among 1983-2005.

Site	Mean annual precipitation (mm)	Dominant Land Cover	Main Soil Texture	Location
1	600-1000	Deciduous shrub land with sparse trees	Oxisols & Entisols	South Sudan
2	600-1000	Cropland (>50%)	Entisols	Nigeria
3	1000-2000	Deciduous woodland	Alfisols	Ghana
4	600-1000	Cropland with open woody vegetation	Alfisols	Borkina Faso &Mali
5	400-1000	Open grassland with sparse shrubs	Alfisols & Entisols	Mali
6	400-600	Cropland (>50%) & Open grassland with sparse shrubs	Entisols	Muritania &Mali

To sum up, cropland with 33.9% and open grasslands by 12.9 % have had the maximum portions of cubic hidden trends (Table.6).

Table.7explains how quadratic trends of LOS related to land cover and soil types over the study area. Quadratic trend of LOS were scattered in north-west of South Sudan, north of Central African Republic and in some small batch areas in Nigeria. The quadratic trends of LOS occured in areas around latitude of 10 degree of north; associated with relatively high annual rainfall, mainly covered by deciduous shrub land, cropland and deciduous woodland.

Table 7. Major land cover covered by quadratic trends. Only the three first main land cover types and soil types which have high percentage of contribution are shown in the table.

3 Main Land Cover classes with Quadratic Trend of LOS (only first three major soil texture types were considered)				
Land Cover	**Mean Annual**	**Soil Texture**	**Percentage**	**Total**

		Precipitation (mm)			Percentage of the trend (including all Soil Textures)
1	Deciduous shrub land with sparse trees	600-1000	Entisols	14.6	28.3
			Alfisols	9.2	
			Ultisols	2.0	
2	Cropland with open woody vegetation	1000-2000	Alfisols	11.3	23.1
			Entisols	7.6	
			Vertisols	2.5	
3	Deciduous woodland	1000-2000	Entisols	7.0	17.2
			Alfisols	4.1	
			Ultisols	3.1	

The cubic trend was found over three small clusters in Central African Republic, Chad and Sudan as shown in Fig. 16C. Deciduous woodland in Central African Republic, deciduous shrub lands with sparse trees in southern Chad and grassland in the border of Chad and Sudan were the main land covers, regarding the occurrence of cubic trend. Negative linear LOS trends occurred in several small patches, mainly located in cropland, in the Sahelian zone.

3.3.3.2. Discussion

The results confirmed that the changes of LOS over the study area could be modeled through higher levels of polynomial trends. The quadratic hidden trends had almost the same notable portion as the linear trend, as shown in the Table. 3. Although the cubic trend could represent the fluctuations of length of growing season well, higher temporal and spatial resolution of the data may have improved the results.

The results of the linear trend analysis showed that the LOS had increased in those areas (Fig. 16C) with relatively high annual rainfall and high greenness, including deciduous woodland and shrub land, cropland and savanna regions. Since no significant changes of amplitude were found over the dominant parts of this area (Fig.16D), the extension of the season might be explained from the seasonal variations in the distribution of rainfall. Also, it might be explained from the soil type of the area; for instance the Oxisols has low degree of fertility which affects the water uptake

by the vegetation roots. However, the results of the positive linear trend analysis confirmed the results of previous research (Hermann et al., 2007, Hermann et al., 2005, Jamali et al., 2014).

The quadratic hidden trend indicates that the area has had the capability to recover, since it has decreased to a short growing season and then increased again The reason for the different magnitude values of the quadratic hidden trends between site number 1, and numbers 2 and 3 (Fig. 29) may be explained by the topography of the area, since number 1 is located in the mountain areas with higher amount of annual rainfall, compared to sites number 2 and 3. The spatial distribution of vertisols in site number 3, which is surrounded by Alfisols, coincided with the spatial distribution of quadratic hidden trend. It was confirmed that the soil type is a determining factor for the fluctuations of vegetation changes in this area.

Regarding the magnitude of the quadratic hidden trends in site number 2; since its main land cover was cropland, a positive magnitude means that the area has had the maximum length of agriculture during the period of 1993 to 1996. The extending of the LOS might be also due to a change in the cultivation of crops over the area.

Deciduous shrub land was the major land cover wherein the higher levels of polynomial could realistically represent changes in LOS. It means that this land cover has had significant variations of the length of growing season, and consequently has been more sensitive to climate changes than other land covers.

Compared to other trend kinds, negative linear trends of LOS had the minimum percentage of LOS changes, only 0.9 % of the entire area. Moreover, the accuracy of the result in these areas is doubtful, due to fairly low value of NDVI, and also due to the difficulty in separating the greenness from noise. Moreover, since the confidence interval of the test was defined as 95% the trend results of low proportion are doubted, particularly for pixels not found in clusters.

Due to cropland has responded strongly to climate variations, LOS has decreased in the cropland regions in the middle part of Ethiopia. .

3.3.4. Polynomial trends of amplitude of season

3.3.4.1. Results

Regarding the amplitude of the season, the negative linear trends (7.9% of the whole study area), positive linear trend (7.3 %), quadratic hidden trend (3.4%) and cubic hidden trend (2.9%) were the main trend kinds found over the study area.

Positive linear trend mainly occurred in the Sahelian zone with low amount of rainfall, while negative linear trends occurred in the Sudanian and Guinean zones with relatively high amount of rainfall (Fig. 16D). While negative linear trends were mainly found in the deciduous woodland and deciduous shrub lands with sparse trees, AMP had increased over the grassland or cropland in the Sahelian zone wherein a relative increase of precipitation was found for the studied period (Huber et al., 2011).

Several clusters of quadratic hidden trend were found in the south-east of South Sudan, Central African Republic and Nigeria. In contrary to cubic trends, quadratic trends more often occurred in clusters, as shown in the Fig. 16D.

The major portion of quadratic hidden trend of AMP was recorded in deciduous woodland, occurring as a large cluster in south and south-east of South Sudan. However, some sparse clusters were found over the west of Central African Republic, Nigeria and some small parts scattered mainly in Guinean zone. Furthermore, results illustrated that the amplitude has reflected the general rainfall pattern over the study area.

3.3.4.2. Discussion

For areas having a negative linear trend of AMP, due to no significant changes of rainfall and soil moisture over these regions for the studied time period (Huber et al., 2011), decrease of amplitude does not seem reasonable. However, the magnitude of the decrease was relatively low as shown in Fig.14D. Nevertheless, the occurance of negative linear trends is fairly consistent with previous findings (Heumann et al., 2007, Jamali et al., 2014, Huber et al., 2011).

In areas with a positive trend of AMP, such as Sudan, increasing the rainfall did not result in significant changes of soil moisture, (Huber et al., 2011). Also, in the absence of soil moisture,

bare soil might have resulted in low NDVI values (Heumann et al., 2007). Thus, the increase was the result of an increase of the total annual rainfall over the area (Heumann et al., 2007).
The quadratic hidden trend of AMP followed the pattern of land cover and soil type as shown in Figs 4, 5 and 6. Deciduous woodland in association with Oxisols soil type coincided with this trend kind. The quadratic trend kind of AMP happened only in the Guinean zone with annual rainfall of more than 1000 mm.

Since the cubic and hidden cubic trends were found as sparse and small clusters over the different zones of study area, they may not represent the real fluctuation of the vegetation phenology.

3.3.5. Polynomial trends of small integral of season

3.3.5.1. Results

Figure (16E) shows trends map of Small Integral of season. Positive linear trend, negative linear trend and hidden quadratic trend were three major trends that found over the study area. However, some small scattered areas of other trend kinds were found over the study area. SI had increased over a large area in the Sahelian and Sudano-Sahelian zones, with precipitation between 400 to 1000 mm, where the lands are dominantly used for agriculture. These areas were found at latitudes higher than 10°N. There were also some patchy areas of positive trend, placed in Central African Republic, South Sudan and Sudan. The trend was coincided fairly well with the distribution of Alfisols.

Negative linear trend was distributed over the South-West part of the study area, including Sierra Leone, Guinea and Coted' Ivoire, which was covered by mosaic forest / cropland. These areas which are close to the equator were classified as areas with high amount of annual precipitation (Guinean zone). There were also some sparse patches in Cameroon and Ethiopia was SI had decreased. Oxisols and Ultisols were the dominant soil types that were associated with the negative linear trend.

Quadratic and cubic trends were limited to some parts of South Sudan, Chad and Nigeria. While the hidden quadratic trend happened in areas with a remarkable fluctuation in SI, the hidden cubic trend were concentrated to the east of Cameroon and some small parts of the South Sudan,

Ethiopia and Central African Republic. The cubic hidden trend did not generally occur in homogeneous soil types. The major land covers where this trend type was found were deciduous woodland, deciduous shrub land and crop lands.

3.3.5.2. Discussion

Regarding linear trends o SI, an increase of the vegetation production was mainly due to a significant increase of rainfall and relative increase in soil moisture over the studied time period (Huber et al., 2011). The rainfall increase led to an increase in NDVI. Since no significant change in length of growing season was recorded over the area (only hidden fluctuations, Fig. 16C), increase the amplitude, resulted in increasing the SI.

Another reason for a negative linear SI trend was the decrease in amplitude. . As discussed in the previous section, due to no changes of NDVI and rainfall, the decreasing in AMP does not seem reasonable. Nevertheless the results were fairly coincident with Heumann et al., (2007).

The quadratic hidden trend of SI can be explained by changes in length of growing season over the related regions. However, the reasons for the fluctuation in LOS varied from one area to another. While the rainfall was expected to be the reason of the quadratic hidden LOS trend in the mountain chain of the western part of Ethiopia, the soil type might have caused the variation of LOS in southern Chad..

3.4 General Discussion

Through computing phenology parameter through 23 years of NDVI data, the general variations of vegetation phenology in the Sahel were identified. Also correlations with soil moisture were identified. Through investigation of mean phenology parameters, it was found that mean SOS and LOS were coincided quite well with rainfall and land cover patterns of the study area. The Guinean zone and mountain areas in Ethiopia had the maximum growing season length.

The results illustrated that linear trends in EOS and LOS mainly increased in the Guinean and Sudano-Sahelian zones, particularly in the Central African Republic and Cameroon, while trends in AMP and SI increased in the Sahelian zone. Linear decreases of SOS, EOS and LOS were

mainly found in the Sahelian zone, while AMP and SI decreased over the Guinean zone. Only AMP had decreased over a vast area, and decreases of SOS, EOS and SI were not substantial compared to their increasing in the Sudano-Sahelian and Guinean zones.

In some areas, higher order polynomial trends revealed vegetation changes better than linear trends because they occurred in clusters. Clustering leads to greater credibility of the results compared to scattered pixels. Furthermore, while there were some areas with significant changes, these changes were not detected either through the linear regressions or the polynomial trends. The hidden polynomial trends detected the fluctuations of vegetation parameters in these areas. However, the magnitude of the polynomial trends (Fig. 12) must be considered in terms of the meaningfulness of the fluctuation because small magnitude of trend is not meaningful.

Since the climatic changes generally occur at large scale, it is important only to interpret changes in phenology parameters occurring in clusters (except in some small irrigated areas), when interpreting cause-and-effects between the climate system and the vegetation. The meaningfulness and magnitude of fluctuation of the parameters must also be considered when interpreting the results.

The results illustrated that the polynomial trends of level 2 (quadratic and hidden quadratic) were more commonly found in clusters than were the cubic trends. The reason might be the low number of investigation years (23 in this case), since more years are needed for identifying statistically significant cubic trends. Also the polynomial of level 2 (quadratic and hidden quadratic trends) mostly occurred around the mountain areas in Ethiopia and central Nigeria (Guinean Zone) with high annual precipitation, while polynomial trends of level 3 (cubic and hidden cubic trends) were scattered in small patches in the Sahelian and Sudano-Sahelian zones (Fig16), with relatively low annual precipitation.

Regarding the correlation between SOS and soil moisture, a moderate negative correlation between SOS and soil moisture was found for the negative linear and hidden quadratic trends in the Sahelian, Sudano-Sahelian and Sudanian zones. Also, soil moisture followed the same trend as SOS. Although, negative moderate correlation between EOS and soil moisture was found in the Sahelian zone, the correlation was positive in the Sudano-Sahelian and Sudanian zones. However,

positive correlations got weaker towards the Guinean zone. While LOS increased in the Sudanian and Guinean zones, cumulative increase of greenness was occurred in the Sudano-Sahelian zone. The reason was due to an increase of the amplitude in this zone, and its decreasing in the Guinean zone. However, as soil moisture dataset has been modelled based on ground based stations, and the distribution of the stations in the study area might not be sufficient, this may have resulted in some inconstancies in the correlations between soil moisture and phenology parameters.

Except in some areas, the vegetation trend changes did not spatially follow land cover and soil types of the study area. However, some land covers and soil types responded more to vegetation changes. Deciduous woodland, shrub lands and irrigated crop lands were those land covers wherein the largest portion of phenology parameter fluctuations were detected. Regarding the soil types, Entisols and Oxisols were the main soil types that were affected, particularly in the Guinean zone.

Uncertainties and Future Work

There were several factors that affected the results, from uncertainties in the remotely sensed data to the extraction of the phenology parameters and application of the trends. Data acquisition and processing errors as well as spatial and temporal resolution of data affected accuracy and precision of extracting the phenology parameters. Lower spatial resolution hides the details of local variability; meanwhile low temporal resolution may not reveal the essential details of growing seasons whereas plant growth is a fairly abrupt change in terms of greenness. Regarding the soil moisture dataset, although the dataset is based on more than 17000 ground stations, the distribution of the stations in the study area might be not sufficient to cover the study area. Also, since the dataset had a coarse spatial resolution compared to the phenology parameters; it might have affected the accuracy of the results. To conclude, in future studies, using more accurate data may give a better perception of how polynomial trends can detect vegetation changes.

Regarding the study area, since there are remarkable variations in climate and geography, a unique extraction method of phenology parameters using the same defined TIMESAT parameters could

not lead to proper extracting of the parameters. For that reason, these characteristic must be taken in consideration in the future works.

Lack of available ancillary data, also not considering variations in a large area and applying only one method of extraction for a large may affect the results, as acknowledged in the linear trend discussion part. However, since no ground based dataset of phenology parameters existed for the study area, the errors could not be properly evaluated. Consequently, using ancillary data and ground based observations must be taken in considerations in future studies.

Furthermore, to analyze the higher polynomial trends particularly cubic and hidden cubic trends may need investigation of longer time periods, because significant fluctuations of changes normally occur in time periods. However, it might be better to use linear trend instead of applying polynomial trends of degree higher than 3, because when the degree of polynomial in a time period increases, magnitudes of fluctuations decrease and trends treats as a linear trend.

3. Conclusion

The results illustrated that polynomial trends can detect notable proportions of vegetation changes in the Sahel using remotely sensed data. Significant portions of areas with linear trends could be represented using quadratic and cubic trends, and these trends increased the precision of phenology change detection. Furthermore, in some areas vegetation changes were not detected neither through linear regressions nor polynomial trends. In these areas, hidden polynomial trends could be applied for detecting the fluctuations of vegetation parameters. Among polynomial trends, hidden quadratic trends covered the largest area. However, these trends were not found over the whole study area. Compared to other zones of the study area, the Sudano-Sahelian zone had the least response to vegetation phenology changes. While LOS increased in the Sudanian and Guinean zones, a cumulative increase of greenness had occurred in the Sudano-Sahelian zone.

The results illustrated how the growing season has shifted in two directions, or, how it was extended or shortened in one or two directions (earlier or later) over the study area. Also, through investigating of quadratic hidden trends, it was realized that LOS increased in specific period of time over some regions, while no changes were recorded in linear trends for these areas.

Regarding the climate driver forces, results showed that the vegetation phenology changes followed soil moisture variations, and in most occurrences, moderate correlations were found between SOS and soil moisture. The trends of vegetation changes did not spatially follow land cover and soil types of the study area. However, in some limited cases, land cover, soil texture and geographic characteristics such as elevation were related to the changes.

To conclude, the most important results of the thesis are:

- Around 95 % of the study area did not experience any changes in SOS, and small portion of the area experienced a linear trend. Nevertheless, quadratic hidden trends with 2.6 % of the whole study area (mostly occurring in clusters) could better detect the changes in SOS.

- EOS and LOS had mainly increased in the Guinean and Sudano-Sahelian zones, while AMP and SI had increased in the Sahelian zone. However, the increase of amplitude did not lead to an extension of the season or any seasonal shift over the area.

- Decrease of SOS, EOS and LOS mainly happened in the Sahelian zone, while AMP and SI decreased over the Guinean zone. However, only AMP had decreased over a vast area (more than one percent per year in Guinea, Côte d'Ivoireand Cameroon), and decrease of SOS, EOS and SI were not substantial compare to their increase in the Sudano-Sahelian and Guinean zones.

- Hidden trends were more efficient in detecting the phenology parameter changes than quadratic and cubic trends. Quadratic hidden trend was the main hidden trend representing large fluctuation of the phenology parameters. This trend mostly occurred in clusters and its main fluctuations occurred from 1993 to 1996.

- Soil moisture was significantly correlated with variation of phenology parameters. However, to analyze the importance of soil moisture it is necessary to investigate more accurate datasets of both soil moisture and precipitation, regarding their spatial and temporal resolutions, over the studied area.

- Although the polynomial trends did not generally follow land cover and soil types of the study area; Entisols and Oxisols were the classes where most phenology changes had occured, particularly in Guinean zone. Also deciduous woodland, shrub lands and irrigated crop lands were those land covers with maximum response to variation in phenology parameters.

- In summation, applying polynomial trend analysis to time-series of satellite data is a powerful tool for investigating trends and variations in vegetation in semi-arid to sub-humid regions, like the Sahel.

5. References

Ahmed, M., 2012, Significance of soil moisture on vegetation greenness in the African Sahel from 1982 to 2008. Master thesis. Department of Physical Geography and Ecosystem Science, Lund University: Sweden.

Anyamba, A., Tucker, C.J., 2005. Analysis of Sahelian vegetation dynamics using NOAA-AVHRR NDVI data from 1981–2003. Journal of Arid Environments, Vol. 63, pp. 596–614.

Badhwar, G.D., 1984.Use of Landsat-derived profile features for spring small-grains classifications. International Journal of Remote Sensing 5:783–797.

Baltzer, H., Gerard, F., George, C., Weedon, G., Grey,W.,Combal,B.,Bartholome,E.,Bartalev, S. and Los,S., 2007.Coupling of vegetation growing season anomalies and fire activity with hemispheric and regional-scale climate patterns in Central and East Siberia. Journal of Climate 20:3713–3729.

Bormann, H., 2012.Assessing the soil texture-specific sensitivity of simulated soil moisture to projected climate change by SVAT modeling. Geoderma 185–186, 73–83.

Bradley, B.A., Jacob, R.W, Hermance, J.F and Mustard, J.F., 2007.A curve-fitting technique to derive interannual phenologies from time series of noisy satellite data, Remote Sensing of Environment, 106,137-145.

Brooks, N., 2004. Drought in the African Sahel: long term perspectives and future prospects. Working Paper 61, Tyndall Centre for Climate Change Research, Norwich, UK.

Cleveland, R.B., Cleveland, W.S., McRae, J.E., and Terpenning, I., 1990. STL: A Seasonal- Trend Decomposition Procedure Based on Loess. Journal of Official Statistics, 6, 3-73.

Chappell, A., Seaquist, J. W. and Eklundh, L., 2001, improving the estimation of noise from NOAA AVHRR NDVI for Africa using geostatistics. International Journal of Remote Sensing, 22, 1067-1080.

Delbart, N., Kergoat, L., Le Toan, T., Lhermittea, J., Picard, G., 2005. Determination of phenological dates in boreal regions using normalized difference water index. Remote Sensing of Environment 97:26–38.

De Beurs, K.M. and Henebry, G.M., 2004.Land surface phenology, climatic variation, and institutional change: analyzing agricultural land cover change in Kazakhstan. Remote Sensing of Environment, 89(4): 497-509.

De Beurs, K.M., and Henebry, G.M., 2010. Phenological research: methods for environmental and climate change analysis, Chapter 9 Spatio-Temporal Statistical Methods for Modelling Land Surface Phenology.Springer, cop. 2010

Eklundh, L., Olsson, L., 2003. Vegetation index trends for the African Sahel 1982–1999.Geophysical Research Letters 30, 1430.

De Jong, R., Verbesselt, J., Schaepman, M.E., de Bruin, S, 2012. Trend changes in global greening and browning: contribution of short-term trends to longer-term change. Global Change Biology, 18, 642-655.

Eklundh, L. and Jönsson, P., 2009. Timesat 3.0: Software Manual, Lund University, Sweden.

Fan Y., H. van den Dool (2004), Climate Prediction Center global monthly soil moisture data set at 0.5° resolution for 1948 to present, Journal of Geophysical Research 109, D10102.

FAO/GIEWS (Food and Agriculture Organization of the United Nations/ Global Information and Early Warning System), 1998.Sahel Report No. 1, Sahel weather and crop situation 1998 http://www.fao.org/giews/english/sahel/index.htm [accessed Feb 2013].

Fensholt, R., Langanke, T., Rasmussen, K., Reenberg, A., Prince, S.D., Tucker, C., Scholes, R.J., Le, Q.B., Bondeau, A., Eastman, R., Epstein, H., Gaughan, A.E., Hellden, U., Mbow, C., Olsson, L., Paruelo, J., Schweitzer, C., Seaquist, J., & Wessels, K., 2012. Greenness in semi-arid areas across the globe 1981–2007 — an Earth Observing Satellite based analysis of trends and drivers. Remote sensing of Environment, 121, 144-158

Fensholt, R.,Rasmussen,K.,Theis N.T., Mbow,C.,2009.Evaluation of earth observation based long term vegetation trends — Intercomparing NDVI time series trend analysis consistency of Sahel from AVHRR GIMMS, Terra MODIS and SPOT VGT data. Remote Sensing of Environment 113, 1886–1898.

Fisher, J.I., Mustard, J.F., Vadeboncoeur, M.A., 2006. Green leaf phenology at Landsat resolution: Scaling from the field to the satellite. Remote Sensing Environment 100,265–279

Fisher, J.I., Mustard J.F., 2007. Cross-scalar satellite phenology from ground, Landsat, and MODIS data. Remote Sensing of Environment. 109, 261-273.

Hall-B.M, 2003. Comparison of single-year and multiyear NDVI time series principal components in cold temperate biomes. Geoscience and Remote Sensing 41, 2568-2574

Haarsma, R. J., Campos, E. J., Hazeleger, W., Severijns, C., Piola, A.R. and Molteni, F., 2005. Dominant modes of variability in the South Atlantic: A study with a hierarchy of ocean-atmosphere models, Journal of Climate, 18, 1719–1735.

Herrmanna, S.M., Anyambab.A. Ukerc.C.J., 2005. Recent trends in vegetation dynamics in the African Sahel and their relationship to climate. Global Environmental Change 15, 394–404

Huete, A.R., 1988. A soil-adjusted vegetation index (SAVI). Remote Sensing of Environment 25, 295–309.

Huber, S., Fensholt, R., Rasmussen, k., 2011.Water availability as the driver of vegetation dynamics in the African Sahel from 1982 to 2007, Global and Planetary Change 76,186–195.

Huete, A., Didan, K., Miura, T., Rodriguez, E.P., Gao, X., Ferreira, L.G., 2002.Overview of the radiometric and biophysical performance of the MODIS vegetation indices. Remote Sensing of Environment.83, 195–213.

Hulme, M., 2001.Climatic perspectives on Sahelian desiccation.1973–1998. Global Environmental Change 11, 19–29.

Held, I. M., Delworth, T. L., Lu, J., Findell, K. L., and Knutson. T. R., 2005.Simulation of Sahel drought in the 20th and 21st centuries, Proceedings of the National Academy of Sciences of the United States of America 102, 17891-17896.

Heumann, B.W., Seaquist, J.W., Eklundh, L. and Jönsson, P., 2007, AVHRR Derived Phenological Change in the Sahel and Soudan, Africa, 1982 - 2005,Remote Sensing of Environment, 108, 385-392.

Jamali, S., Seaquist, j., Eklundh, L., Ardö, J., Accurate, 2014, automated mapping of long-term vegetation trends with polynomials using NDVI imagery over North Africa. Remote Sensing of Environment 141, 79–89.

James ME, Kalluri SNV., 1994.The Pathfinder AVHRR Land data set - an improved coarse resolution data set for terrestrial monitoring. International Journal of Remote Sensing 15, 3347–3363.

Jan Verbesselt, Rob Hyndman, Glenn Newnham, Darius Culvenor, 2010. Detecting Trend and Seasonal Changes in Satellite Image Time Series. Remote Sensing of Environment, 114(1), 106-115

Jeong, S. J., Ho, C.H., Gim, H. J., & Brown, M. E. (2011). Phenology shifts at start vs. end of growing season in temperate vegetation over the Northern Hemisphere for the period 1982–2008. Global Change Biology. http://dx.doi.org/10.1111/j.1365-2486.2011.02397.x

Julien, Y., Sobrino, J.A., 2009.The Yearly Land Cover Dynamics (YLCD) method: An analysis of global vegetation from NDVI and LST parameters, Remote Sensing of Environment 113, 329–334.

Jönsson, P. and Eklundh, L., 2002, Seasonality extraction and noise removal by function fitting to time-series of satellite sensor data, IEEE Transactions of Geoscience and Remote Sensing, 40, No 8, 1824 – 1832.

Jönsson, P. and Eklundh, L., 2004, Timesat - a program for analyzing time-series of satellite sensor data, Computers and Geosciences, 30, 833 – 845.

Jönsson, P. and Eklundh, L., 2002, Seasonality extraction and noise removal by function fitting to time-series of satellite sensor data, IEEE Transactions of Geoscience and Remote Sensing, 40, No 8, 1824 – 1832.

Jönsson, P. and Eklundh, L., 2004, Timesat - a program for analyzing time-series of satellite sensor data, Computers and Geosciences, 30, 833 – 845.

Justice, C. O., Townshend, J. R. G., Holben, B. N., & Tucker, C. J., 1985.Analysis of the phenology of global vegetation using meteorological satellite data. International Journal of Remote Sensing, 6, 1271 ± 1318.

Jakubauskas, M. E., Peterson, D.L., Kastens, J.H. and Legates, D. R., 2002.Time series remote sensing of landscape-vegetation interactions in the southern Great Plains, Photogrammetric Engineering and Remote Sensing, 68, 1021-1030.

Karlsen SR, Elvebakk A, Hogda KA et al., 2006. Satellite-based mapping of the growing season and bioclimatic zones in Fennoscandia. Global Ecol Biogeogr 15:416–430

Karlsen SR, Solheim I, Beck PSA et al., 2007. Variability of the start of the growing season in Fennoscandia, 1982–2002. Int J Biometeorol 51:513–524.

Karlsen, S.R., Tolvanen, A.,Kubin,E., Poikolainen, J.,Høgda, ., K.A. , Johansen,B., Danks, F. S., Aspholm, P., Wielgolaski, F. E. and Makarova,O., 2008. MODIS-NDVI based mapping of the length of the growing season in northern Fennoscandia. International Journal of Applied Earth Observation and Geoinformation, 10: 253-266.

Kaufman, Y.J., Tanre, D., 1992. Atmospherically resistant vegetation index (ARVI) for EOS-MODIS. IEEE Transactions of Geoscience and Remote Sensing 30, 261–270.

Kogan, F.N., 1995.Droughts of the late 1980's in the United States as derived from NOAA polarorbiting satellite data. Bull American Meteorological Society 76,655–668.

Kandji, S.T., Verchot, L. and, Mackensen, J., 2006.Climate Change Climate and Variability in Southern Africa: Impacts and Adaptation in the Agricultural Sector, Copyright © UNEP & ICRAF.

Kumar, L., Rietkerk, M., Langevelde, F.V., 2002, Relationship between vegetation growth rates at the onset of the wet season and soil type in the Sahel of Burkina Faso: implications for resource utilisation at large scales. Ecological Modelling 149,143–152

Le Houerou, H.H., 1977. Man and desertization in the Mediterranean region. Ambio (Sweden) 6, 363–365.

Le Houerou, H.N., 1980. The range lands of the Sahel. Journal of Range Management, Vol.33, 41–46.

Lloyd, D., 1990.A phenological classification of terrestrial vegetation cover using shortwave vegetation index imagery. International Journal of Remote Sensing, 11, 2269 ± 2279.

Moody, A. and Johnson, D. M., 2001, Land-Surface Phenologies from AVHRR Using the Discrete Fourier Transform, Remote Sensing of Environment, 75, 305-323.

Maignan, F., Bréon, M., Bacour, C., Demarty, j., Poirson, A., 2008.applications. Remote sensing of Environment 112,496-505.

Montandon, L.; Small, E., 2008.The impact of soil reflectance on the quantification of the green vegetation fraction from NDVI. Remote Sens. Environ 112, 1835–1845.

Myneni, R.B., Hall, F.G., Sellers, P.J., Marshak, A.L., 1995.The interpretation of spectral vegetation indexes. IEEE Transactions on Geoscience and Remote Sensing, 33, 481–486.

Moulin, S., L. Kergoat, N. Viovy, and G. Dedieu., 1997.Global-scale assessment of vegetation Phenology using NOAA/AVHRR satellite measurements, Journal of Climate, 10, 1154-1170.

Mugalavai, E.M., Kipkorir, E.C., Raes, D., Rao, M.S., 2008.Analysis of rainfall onset, cessationand length of growing season for western Kenya. Agricultural and Forest Meteorology 148, 1123–1135

McCloy, K. R., Los, S., Lucht, W., & Hojsgaard, S., 2005. A comparative analysis of three long-term NDVI datasets derived from AVHRR satellite data. EARSeL eProceedings 4, 52−69.

Mitchell, T., Hulme, M., 1999.Predicting regional climate change: living with uncertainty. Progress in Physica Geography 23, 57–78.

Naden, P.S., Watts, C.D., 2001. Estimating climate-induced change in soil-moisture at the landscape scale: an application to five areas of ecological interest in the UK. Climatic Change 49, 411–440.

Nicholson.S., 2005.On the question of the "recovery" of the rains in the West African Sahel. Journal of Arid Environments 63, 615–641.

Norman K., Janssen, L.L.F. and Huurneman.G.C, 2004.Principles of Remote Sensing. (ITC Educational Textbook Series; 2). The International Institue for Geo-Information Science and Earth Observation (ITC), Enschede, the Netherlands.

Olsson L. and Eklundh L. (1994) Fourier transformation for analysis of temporal sequences of satellite imagery. *International Journal of Remote Sensing* 15, 3735-3741.

Olsson, L., Eklundh, L., Ardoe, J., 2005. A recent greening of the Sahel—trends, patterns, and potential causes. Journal of Arid Environments 63, 556–566.

Pedelty J, Devadiga S, Masuoka E et al. 2007.Generating a long-term land data record from the AVHRR and MODIS Instruments. In: Geoscience and Remote Sensing Symposium IGARSS.

Petra T., 2007.Views from the vulnerable: Understanding climatic and other stressors in the Sahel. Global Environmental Change 17, 381–396.

Qi, J., Chehbouni, A., Huete, A.R., Kerr, Y.H., Sorooshian, S., 1994. A modified soil adjusted vegetation index. Remote Sensing of Environment 48, 119–126.

Rasmussen, K., Fog, B., Madsen, J.E., 2001. Desertification in reverse? Observations from northern Burkina Faso. Global Environmental Change 11, 271–282.

Reed, B. C., Brown, J. F., VanderZee, D., Loveland, T. R., Merchant, J. W. and Ohlen, D. O., 1994.Measuring phenological variability from satellite imagery. Journal of Vegetation Science 5,703–714.

Reed, B.C.; Schwartz, M.D.; Xiao, X., 2009. Remote Sensing Phenology: Status and the Way Forward In Phenology of Ecosystem Processes; Springer: New York, NY, USA, 231–246.

Rouse J. W., Haas, R. H., Deering, and D. W., Sehell, J.A., 1974.Monitoring the vernal advancement and retro gradation (Green wave effect) of natural vegetation. Final Rep. RSC 1978-4, Remote Sensing Center, Texas A&M Univ., and College Station.

Seaquist J.W., Hickler T., Eklundh L., Ardö J. and Heumann B. (2009) Disentangling the effects of climate and people on sahel vegetation dynamics. Biogeosciences 6, 469-477.

Shabanov N.V., Zhou ,L., Knyazikhin,Y., Myneni R.B., and Tucker C.J.,2002 .Analysis of interannual changes in northern vegetation activity observed in AVHRR data during 1981 to 1994, IEEE Transactions on Geoscience and remote sensing 40:115-130.

Tateishi, R., Ebata, M., 2004.Analysis of phenological change patterns using 1982–2000 Advanced Very High Resolution Radiometer (AVHRR) data. International Journal of Remote Sensing 25, 2287–2300.

Tso, B. and Mather, P.M., 2009.Classification Methods for Remotely Sensed Data (Second edition). Abingdon: CRC Press, 376 pp.

Tucker, C.J., Pinzon, J.E., Brown, M.E.,Slayback,D., Pak, E., Mahoney, R., Vermote, E., El Saleous, N. , 2005.An extended AVHRR 8-km NDVI dataset compatible with MODIS and SPOT vegetation NDVI data. International Journal of Remote Sensing 26, 4485–4498.

Tucker, C.J., Nicholson, S.E., 1999. Variations in the size of the Sahara desert from 1980 to 1997. Ambio 28, 587–591.

Verbesselt, J., Hyndman, R., Newnham, G. & Culvenor, D., 2010. Detecting trend and seasonal changes in satellite image time series. Remote Sens Environ 114, 106–115.

Verbesselt, J., Hyndman, R., Zeileis,A., Culvenor.D., 2010.Phenological Change Detection while Accounting for Abrupt and Gradual Trends in Satellite Image Time Series. Remote Sensing of Environment, 114, 2970 – 2980.

White, M.A., Thornton, P.E., Running, S.W., 1997. A continental phenology model for monitoring vegetation responses to interannual climatic variability. Global Biogeochemectry 11, 217–234.

White, M.A. and Nemani, R.R., 2006, Real-time monitoring and short-term forecasting of land surface phenology. Remote Sensing of Environment, 104, pp. 43–49.

Xiao, X., Hollinger, D., Aber, J. D., Goltz, M., Davidson, E. A., & Zhang, Q. Y. (2004).Satellite-based modeling of gross primary production in an evergreen needleleaf forest.Remote Sensing of Environment, 89,519 – 534.

Zhang, X., Friedla, M.A., Schaaf, C.B., Strahlera, A.H., Hodgesa, J.C.F, Gaoa, F., Reedb, B.C., Huetec, A., 2003.Short communication Monitoring vegetation phenology using MODIS, Remote Sensing of Environment 84, 471 – 475.

Zhang, X., Friedl, M.A., Schaaf, C.B.,Strahler, A.H.,2004 .Climate controls on vegetation phenological patterns in northern mid- and high latitudes inferred from MODIS data. Global Change Biology 10:1133–1145.

Seminar Series

Institutionen för naturgeografi och ekosystemvetenskap, Lunds Universitet.

Student examensarbete (Seminarieuppsatser). Uppsatserna finns tillgängliga på institutionens geobibliotek, Sölvegatan 12, 223 62 LUND. Serien startade 1985. Hela listan och själva uppsatserna är även tillgängliga på LUP student papers (www.nateko.lu.se/masterthesis) och via Geobiblioteket (www.geobib.lu.se)

The student thesis reports are available at the Geo-Library, Department of Physical Geography and Ecosystem Science, University of Lund, Sölvegatan 12, S-223 62 Lund, Sweden. Report series started 1985. The complete list and electronic versions are also electronic available at the LUP student papers (www.nateko.lu.se/masterthesis) and through the Geo-library (www.geobib.lu.se)

245 Linnea Jonsson (2012). Impacts of climate change on Pedunculate oak and Phytophthora activity in north and central Europe

246 Ulrika Belsing (2012) Arktis och Antarktis föränderliga havsistäcken

247 Anna Lindstein (2012) Riskområden för erosion och näringsläckage i Segeåns avrinningsområde

248 Bodil Englund (2012) Klimatanpassningsarbete kring stigande havsnivåer i Kalmar läns kustkommuner

249 Alexandra Dicander (2012) GIS-baserad översvämningskartering i Segeåns avrinningsområde

250 Johannes Jonsson (2012) Defining phenology events with digital repeat photography

251 Joel Lilljebjörn (2012) Flygbildsbaserad skyddszonsinventering vid Segeå

252 Camilla Persson (2012) Beräkning av glaciärers massbalans – En metodanalys med fjärranalys och jämviktslinjehöjd över Storglaciären

253 Rebecka Nilsson (2012) Torkan i Australien 2002-2010 Analys av möjliga orsaker och effekter

254 Ning Zhang (2012) Automated plane detection and extraction from airborne laser scanning data of dense urban areas

255 Bawar Tahir (2012) Comparison of the water balance of two forest stands using the BROOK90 model

256 Shubhangi Lamba (2012) Estimating contemporary methane emissions from tropical wetlands using multiple modelling approaches

257 Mohammed S. Alwesabi (2012) MODIS NDVI satellite data for assessing drought in Somalia during the period 2000-2011

258 Christine Walsh (2012) Aerosol light absorption measurement techniques:
A comparison of methods from field data and laboratory experimentation

259 Jole Forsmoo (2012) Desertification in China, causes and preventive actions in modern time

260 Min Wang (2012) Seasonal and inter-annual variability of soil respiration at Skyttorp, a Swedish boreal forest
261 Erica Perming (2012) Nitrogen Footprint vs. Life Cycle Impact Assessment methods – A comparison of the methods in a case study.
262 Sarah Loudin (2012) The response of European forests to the change in summer temperatures: a comparison between normal and warm years, from 1996 to 2006
263 Peng Wang (2012) Web-based public participation GIS application – a case study on flood emergency management
264 Minyi Pan (2012) Uncertainty and Sensitivity Analysis in Soil Strata Model Generation for Ground Settlement Risk Evaluation
265 Mohamed Ahmed (2012) Significance of soil moisture on vegetation greenness in the African Sahel from 1982 to 2008
266 Iurii Shendryk (2013) Integration of LiDAR data and satellite imagery for biomass estimation in conifer-dominated forest
267 Kristian Morin (2013) Mapping moth induced birch forest damage in northern Sweden, with MODIS satellite data
268 Ylva Persson (2013) Refining fuel loads in LPJ-GUESS-SPITFIRE for wet-dry areas - with an emphasis on Kruger National Park in South Africa
269 Md. Ahsan Mozaffar (2013) Biogenic volatile organic compound emissions from Willow trees
270 Lingrui Qi (2013) Urban land expansion model based on SLEUTH, a case study in Dongguan City, China
271 Hasan Mohammed Hameed (2013) Water harvesting in Erbil Governorate, Kurdistan region, Iraq - Detection of suitable sites by using Geographic Information System and Remote Sensing
272 Fredrik Alström (2013) Effekter av en havsnivåhöjning kring Falsterbohalvön.
273 Lovisa Dahlquist (2013) Miljöeffekter av jordbruksinvesteringar i Etiopien
274 Sebastian Andersson Hylander (2013) Ekosystemtjänster i svenska agroforestrysystem
275 Vlad Pirvulescu (2013) Application of the eddy-covariance method under the canopy at a boreal forest site in central Sweden
276 Malin Broberg (2013) Emissions of biogenic volatile organic compounds in a Salix biofuel plantation – field study in Grästorp (Sweden)
277 Linn Renström (2013) Flygbildsbaserad förändringsstudie inom skyddszoner längs vattendrag
278 Josefin Methi Sundell (2013) Skötseleffekter av miljöersättningen för natur- och kulturmiljöer i odlingslandskapets småbiotoper
279 Kristín Agustsdottír (2013) Fishing from Space: Mackerel fishing in Icelandic waters and correlation with satellite variables
280 Cristián Escobar Avaria (2013) Simulating current regional pattern and composition of Chilean native forests using a dynamic ecosystem model
281 Martin Nilsson (2013) Comparison of MODIS-Algorithms for Estimating

Gross Primary Production from Satellite Data in semi-arid Africa

282 Victor Strevens Bolmgren (2013) The Road to Happiness – A Spatial Study of Accessibility and Well-Being in Hambantota, Sri Lanka

283 Amelie Lindgren (2013) Spatiotemporal variations of net methane emissions and its causes across an ombrotrophic peatland - A site study from Southern Sweden

284 Elisabeth Vogel (2013) The temporal and spatial variability of soil respiration in boreal forests - A case study of Norunda forest, Central Sweden

285 Cansu Karsili (2013) Calculation of past and present water availability in the Mediterranean region and future estimates according to the Thornthwaite water-balance model

286 Elise Palm (2013) Finding a method for simplified biomass measurements on Sahelian grasslands

287 Manon Marcon (2013) Analysis of biodiversity spatial patterns across multiple taxa, in Sweden

288 Emma Li Johansson (2013) A multi-scale analysis of biofuel-related land acquisitions in Tanzania - with focus on Sweden as an investor

289 Dipa Paul Chowdhury (2013) Centennial and Millennial climate-carbon cycle feedback analysis for future anthropogenic climate change

290 Zhiyong Qi (2013) Geovisualization using HTML5 - A case study to improve animations of historical geographic data

291 Boyi Jiang (2013) GIS-based time series study of soil erosion risk using the Revised Universal Soil Loss Equation (RUSLE) model in a micro-catchment on Mount Elgon, Uganda

292 Sabina Berntsson & Josefin Winberg (2013) The influence of water availability on land cover and tree functionality in a small-holder farming system. A minor field study in Trans Nzoia County, NW Kenya

293 Camilla Blixt (2013) Vattenkvalitet - En fältstudie av skånska Säbybäcken

294 Mattias Spångmyr (2014) Development of an Open-Source Mobile Application for Emergency Data Collection

295 Hammad Javid (2013) Snowmelt and Runoff Assessment of Talas River Basin Using Remote Sensing Approach

296 Kirstine Skov (2014) Spatiotemporal variability in methane emission from an Arctic fen over a growing season – dynamics and driving factors

297 Sandra Persson (2014) Estimating leaf area index from satellite data in deciduous forests of southern Sweden

298 Ludvig Forslund (2014) Using digital repeat photography for monitoring the regrowth of a clear-cut area

299 Julia Jacobsson (2014) The Suitability of Using Landsat TM-5 Images for Estimating Chromophoric Dissolved Organic Matter in Subarctic Lakes

300 Johan Westin (2014) Remote sensing of deforestation along the trans-Amazonian highway

301 Sean Demet (2014) Modeling the evolution of wildfire: an analysis of

short term wildfire events and their relationship to meteorological variables

302 Madelene Holmblad (2014). How does urban discharge affect a lake in a recreational area in central Sweden? – A comparison of metals in the sediments of three similar lakes

303 Sohidul Islam (2014) The effect of the freshwater-sea transition on short-term dissolved organic carbon bio-reactivity: the case of Baltic Sea river mouths

304 Mozafar Veysipanah (2014) Polynomial trends of vegetation phenology in Sahelian to equatorial Africa using remotely sensed time series from 1983 to 2005